DURABILITY STUDY OF BASALT FIBER-REINFORCED BARS EXPOSED TO HARSH ENVIRONMENTS

by

Mohamad Mazen Alrifai

A Thesis presented to the Faculty of the
American University of Sharjah
College of Engineering
In Partial Fulfillment
of the Requirements
for the Degree of

Master of Science in
Civil Engineering

Sharjah, United Arab Emirates

April 2019

Approval Signatures

We, the undersigned, approve the Master's Thesis of Mohamad Mazen Alrifai

Thesis Title: Durability Study of Basalt Fiber-reinforced Bars Exposed to Harsh Environments.

Signature	**Date of Signature** (dd/mm/year)
_____ Dr. Farid Abed Professor, Department of Civil Engineering Thesis Advisor	_____
_____ Dr. Tamer El Maaddawy Professor, Department of Civil and Env. Engineering, UAEU Thesis Co-Advisor	_____
_____ Dr. Sherif Mohamed Ahmed Professor, Department of Civil Engineering Thesis Committee Member	_____
_____ Dr. Noha Mohamed Hassan Hussein Associate Professor, Department of Industrial Engineering Thesis Committee Member	_____
_____ Dr. Irtishad U. Ahmad Head, Department of Civil Engineering	_____
_____ Dr. Lotfi Romdhane Associate Dean for Graduate Affairs and Research College of Engineering	_____
_____ Dr. Naif Darwish Acting Dean, College of Engineering	_____
_____ Dr. Mohamed El-Tarhuni Vice Provost for Graduate Studies	_____

Acknowledgement

I would like to thank my advisors Dr. Farid Abed and Dr. Tamer Al-Maadawy for providing knowledge, guidance, support, and motivation throughout my research stages. I'm deeply beholden for their great assistance, worthy discussion and suggestions. I would like to thank the following professors and instructors for the assistance:

- Dr. Hilal ElHassan /UAEU
- Mr. Arshi Faridi /AUS
- Mr. Abdelrahman Elsallamin /UAEU
- Mr. Nizam Aldin /UAEU
- Mr. Bassam /UAEU
- Mr. Ehab Elsaid /UAEU
- Mr. Salem /UAEU
- Mr. Yazan Al-Houbi /AUS

I would like to thank the professors of the Civil Engineering department who taught me the master level courses with mighty teaching methods and skills. I really appreciate their dignified advices and motivation. I would also like to thank the American University of Sharjah for providing me a teaching assistantship during my graduate studies.

Abstract

In this research, the durability of Basalt Fiber Reinforced Polymers (BFRP) bars of 10 mm diameter is studied after direct exposure to severe conditions. The main aim is to investigate the degradation performance of the microstructure and tensile properties of these BFRP bars under accelerated conditionings that simulate the concrete's environment. A set of BFRP bars was wrapped by concrete prisms that were immersed in tap water. Another set of BFRP bars was exposed to alkaline solution. In concrete-wrapped and alkaline exposures, temperatures of 20^{o}C, 40^{o}C, 60^{o}C were applied in isolated tanks for durations of 2880, 5760, and 8760 hours. The experimental program included Uniaxial Tensile Tests, Scanning Electron Microscopy (SEM), Water Absorption, Differential Scanning Calorimetry Analysis (DSC), Fourier Transform Infrared Spectrometry (FTIR), Matrix Digestion, and Fiber Volume Fraction Analysis. This combination of tests was selected to validate the tensile strength values. The output of these tests is a comprehensive microstructural characterization and tensile behavior evaluation before and after exposure to harsh environments. As a result, the effect of temperature was more distinct than the effect of exposure periods. Higher temperatures and greater durations in a harsh environment tend to cause impairments on the structural and microstructural levels. These impairments are represented by tensile loss, debonding, matrix loss, moisture impregnation, and micro-cracking at the fiber-matrix interface. Maximum tensile loss, moisture loss, and matrix loss were recorded to be 29%, 1%, 29.8%, respectively, for the samples that were conditioned for 9 months at 60^{o}C in alkaline environment.

Keywords: ***fiber-matrix interface; hydrolysis; scanning electron microscopy; degradation.***

Table of Contents

List of Figures

List of Tables

Chapter 1. Introduction

Fiber-reinforced polymers (FRP) can be defined as continuous composite fibers which are impregnated into a binding mold with resin supply, where the resulting composites are to be cured and shaped as desired [1]. FRP composites became a convenient alternative to conventional steel due to its eco-friendly properties and high structural performance. The most commonly used FRP composites are Carbon (CFRP), Glass (GFRP), Aramid (AFRP), and recently the Basalt (BFRP). The new BFRP bars proved its competence to the various types of FRP composites because of its remarkable properties that will be mentioned and discussed in the following sections [1]. The main properties of BFRP include: high durability performance, tensile strength, creep behavior, strength/weight ratio, thermal non-conductivity, and stiffness [2, 3, 4, 5].

1.1. Types of FRP

FRP are typically produced by a process called Pultrusion, bonding three different unidirectional layers in different orientation to increase the composite reaction [2]. The FRP composites are classified and named based on the fiber material such as GFRP, CFRP, AFRP and the most recent the BFRP. Figure 1-1 shows the different types of FRP bars developed based on fiber-composites in addition to steel bars. The proposed investigation mainly discusses the durability of Basalt FRP exposed to harsh environments, and how the harsh conditioning might affect the macro-mechanical and micromechanical behavior of these BFRP bars. Each type of FRP composite has a certain coefficient of thermal expansion (transverse and longitudinal) which plays a critical role in durability performance and bonding strength. A brief description of production process, general composition, and mechanical properties indications of BFRP and GFRP is provided in the following sections.

1.1.1. GFRP. GFRP composite is composed of high strength fibers that are bonded harmonically to provide the highest composite reaction. The fibers are made of four main types; E-glass, S-glass, C-glass, and AR- glass. As mentioned previously, the production is implemented by a process called Pultrusion which is the most commonly used production process. It includes the binding of fibers by a certain type of resin, thermosetting or thermoplastic resins, then the bonded fibers are die-cured by heat. The extracted composites are mostly structural shapes (e.g. I-beam, boxes, and channels).

Various types of surface treatments or curing such as sand coating, roughing, continuous thread, and forming are applied on the GFRP bars in order to increase the bonding strength in contact with concrete [9]. The mechanical properties of GFRP has a range of 483 to 1600 MPa of tensile strength and 35 to 51 GPa of elastic modulus, with a range of density between 1.25 and 3.1 g/cm³ density [1].

Figure 1-1: From left to right: ribbed steel bars, ribbed AFRP, ribbed CFRP, sand-coated CFRP, grooved GFRP, sand-coated GFRP bars, ribbed BFRP bars, and sand-coated Basalt FRP bars [6, 7, 8].

1.1.2. BFRP. Basalt rocks are volcanic dark rocks made from rapidly-cooled lava. The Basalt fibers are extracted from the Basalt rocks and manufactured via Pultrusion similar to the production concept of GFRP composites. However, the energy consumed in the manufacturing process of BFRP is less which grants the BFRP composites environmental and economic privileges. Due to its excellent properties regarding tensile strength, fire resistance, non-corrosive nature, environmental confrontation, and strength/weight ratio, the BFRP composites has emerged as a promising replacement of the conventional steel bars [10]. BFRP and GFRP possess a similar modulus of elasticity of around 50 GPa. Table 1-1 illustrates the difference in chemical composition between E-glass and basalt materials [11].

1.2. Properties of FRP

What makes FRP better than conventional structural composites are the advanced properties it demonstrates when compared to other composite materials.

Table 1-1: Percentages of certain chemical compounds in R-glass and basalt fibers [11].

Compound	SiO_2	Al_2O_3	CaO	MgO	B_2O_3	Na_2O_3	K_2O	Fe_2O_3
% in E-glass	52-56	12.1-16.1	16-25	0-5	1.3-3.7	0.8	0.2-0.8	≤0.3
% in Basalt	51.6-57.5	16.9-18.2	5.2-7.8	5.1-10.1	-	2.5-6.4	0.8-4.5	4.0-9.5

1.2.1. Tensile strength. The tensile strength of FRP is greatly high due the type of fiber reinforcement such as E-glass with 750 MPa to 1050 MPa tensile strength, Aramid (1150 MPa to 1400 MPa), Carbon-pitch (1400 MPa to 1500 MPa), etc. These composites are manufactured using a synthetic process called "Pultrusion" [5].

1.2.2. Low density. In general, the density of FRP is around two third less than concrete and one fifth less than steel. For example, the glass fiber reinforced polymer density ranges from 1750 kg/m to 1850 kg/m^3 while the steel density ranges from 7800 kg/m^3 to 8000 kg/m^3. As a result, using FRP reduces the transportation cost as well as the labor cost [3].

1.2.3. Thermal non-conductivity. The thermal conductivity is an important factor that can affect any construction material, the thermal conductivity of FRP materials is very low which may be considered as a non-conductive (insulating) material since the polymer has a very low conductivity [4].

1.2.4. Lightweight and stiffness. FRP composites reduce the dead loads of the structure significantly. For instance, the weight of FRP-reinforced concrete (RC) bridge deck is about 20% of the conventional steel-RC bridge deck. However, it has a lower stiffness than the conventional one [2].

1.3. Problem Statement

To overcome the deficiencies of conventional steel, BFRP bars are used in the industry due to its superior mechanical and environmental properties. The high chemical confrontation and corrosion resistance make BFRP bars an ideal replacement for conventional steel. By embedding BFRP bars into a concrete system, it's overall structural integrity will be maintained. Therefore, using BFRP bars as reinforcements in concrete structures within the Middle East suggests a practical approach in preventing accelerated deterioration due to the severe climate conditions [3, 4].

1.4. Research Significance

BFRP bars are introduced to the construction industry as a feasible alternative to carbon FRP and glass FRP bars, possessing remarkable environmental and economic characteristics with excellent tensile, shear, and bond properties. In order to implement

BFRP bars in the construction industry, the durability and degradation performance of the bars should be investigated thoroughly by subjecting them to harsh environmental conditioning within a certain duration. The study of durability testing for BFRP bars will serve as a reliable source in the research community due to its applications in maintaining structural integrity and serviceability of structures. This thesis presents an experimental investigation of the durability of BFRP bars subjected to severe conditions.

1.5. Research Objectives

The objectives of this research study can be summarized as follows:

1. To evaluate the durability and degradation behavior of BFRP bars exposed to harsh accelerated environments isolated in temperature-controlled tanks, considering moist concrete-wrapped BFRP bars.
2. To investigate the effect of alkaline on the durability and degradation performance of BFRP.
3. To study the effect of temperature and exposure period variations on the durability and degradation performance of BFRP.
4. To perform an extensive testing program before and after conditioning, and study the durability performance and microstructures; including Scanning Electron Micrographs (SEM), Water Absorption, Differential Scanning Calorimetry Analysis (DSC), Fourier Transform Infrared (FTIR) Spectrometry, Matrix Digestion, and Fiber Volume Fraction Analysis.

1.6. Thesis Structure

The rest of the thesis is organized as follows: Chapter 2 provides background about FRP composites durability and degradation performance, when exposed to different kinds of exposures. Moreover, related works to this research are discussed. The employed methods and tests are discussed in Chapter 3 along with an overview of the materials properties, conditioning setup, and testing procedures and deliverables. Chapter 4 presents the results of the study along with a compressive discussion and verification with other recent studies, Chapter 5 concludes the thesis and outlines the future work.

Chapter 2. Literature Review

FRP composites feature a non-corrosive nature and high strength-to-weight ratio over other structural rebar materials that have been previously used [5, 6, 7, 8, 9, 10]. The BFRP, produced from natural volcanic rocks, is eco-friendly, recyclable, has lower embodied energies, and a lower cost [12, 13, 14]. Hence, BFRP became a popular material in different civil engineering applications such as: infrastructure, superstructures, and energy facilities due to its high strength and chemical resistance [15].

There are many studies conducted on the durability of CFRP, GFRP, and BFRP by many authors, scientists, and senior engineers. These studies targeted the durability and bond properties of Carbon FRP exposed to harsh environments, such as seawater [16, 17, 18].

The durability and degradation behavior of GFRP bars exposed to severe environments, like moist concrete, have been investigated. However, the studies included short-term exposure along with long-term durability prediction modeling [19, 20, 21]. These studies focused on the durability and degradation of BFRP subjected to various, temperature-controlled, and harsh conditions such as: saline, acidic, and alkaline environments, where the temperature was the main accelerating factor [13, 22, 23, 24]. Some studies focused on the shear behavior of BFRP and GFRP bars in beams, where the varying parameters were beam reinforcement and geometry [25, 26]. In addition, many studies were conducted to investigate the effect of harsh exposures on the bond capacity between the concrete and FRP reinforcement [27, 28]. Other studies focused on the effect of BFRP reinforcement on the shear behavior of deep beams [29]. Abed et al. [30] conducted an experimental investigation on the effect of BFRP reinforcement on the flexural capacity of beams.

2.1. Durability and Degradation Behavior of FRP Composites

The Gulf region exhibits harsh environments which attack the corrosive reinforcing steel bars severely, causing disintegrity of the structural behavior and serviceability; thus, leading to safety hazards and financial losses due to continuous maintenance. Non-metallic and noncorrosive materials could be used as a replacement

of conventional reinforcements which can resist efficiently the harsh chemical attack that is accompanied with chlorides, sulfates, and carbons etc. The use of such materials prolongs the service lives and durability and reduces the safety risks and vital maintenance costs. A recent manufacturing process created a new material technology which is based on nonmetallic fibers. GFRP and BFRP have shown remarkable mechanical properties along with the high endurance to harsh environments. Unlike the steel bars, the fiber-reinforced composites durability depends on many factors associated with the fibers and resin properties such as; the surface finish of bars, bond mechanism, resin type and quality, and the presence of micro-cracks in resins. Also, other factors that are linked to the curing of concrete and the good surface finish which promotes an affective concrete cover [7].

A comparative study was conducted on the glass/Vinylester, Basalt/Vinylester, and basalt/Epoxy (Fiber type/different resin compounds) by Benmokrane et al. [31]. The experimental program included a physical characterization of bar samples before conditioning, transition temperatures, fiber content, and resin density. It also included different types of exposure to alkaline, water, saline, and acidic to simulate concrete exposure for different durations and temperatures. Mass loss and moisture uptake in each environment were studied between 1 and 7 days. The conditioning durations were 1000, 3000, 5000 hours. It was observed that acidic solutions were the most influential, causing up to 6% mass loss. The pilot investigation was conducted to provide a simulation of how the chemicals would affect the basalt fibers. Physical, chemical, mechanical, and durability characteristics of each FRP composite was studied. As a result, B/V bars were highly affected by the alkaline solution accelerated aging resulting in a shear strength reduction of around 33% after 5000 hours at 60ºC. However, the G/V and B/E bars were barely affected by approximately 10% transverse shear reduction. The flexural strength of B/V and B/E was reduced by 37% and 39% respectively after 5000 hours of conditioning, while the G/V experienced a less reduction of only 7%.

Li et al. [32] studied the BFRP feasibility as an alternative of GFRP and CFRP by focusing on the hygrothermal and alkaline environments without resin protection. Seven-mm diameter BFRP bars, with a fiber content of 72%, were cut into 30 mm samples. The samples were soaked in water, alkaline, and natural ambient (23ºC and

30% relative humidity) environments at 20ºC, 40ºC, 60ºC, and 80ºC for 30 days duration. Service lives were predicted using Arrhenius equations, where it was observed that the BFRP bars absorption rate was higher in alkaline solutions. However, they showed a poor alkali resistance and experienced a high reduction in both tensile strength and modulus compared with distilled water resistance. Scanning Electron Microscope (SEM) analysis showed the hydrolysis and debonding of resin, which effectively influenced the degradation rate in alkaline solution.

Wang and GangaRao [33] studied the behavior of fiber reinforced polymer exposed to moisture, temperature, sustained stress, and ultraviolet radiation. Predictive models were adopted with application potential and limitations such as: diffusion model, three-dimensional Fickian model, two-stage model, and Langmuir's model etc. The Review concluded that the pH variations influenced the FRP strength more than its stiffness. Extreme acid environments seemed to be more damaging than extreme alkaline environments except for glass FRP. Moreover, the review revealed that the most aggressive factor which lowered the tensile strength and increased the moisture absorption rate was the high temperature. As a result, the UV radiation exposure along with high-temperature caused a severe degradation in the matrix and fiber levels.

Furthermore, most of the recent studies focused on FRP resistivity to corrosive environments, whereas very limited studies targeted the durability of BFRP bars in alkaline and other extreme environments. In addition, no comprehensive studies have been found on the durability and degradation of Epoxy-based BFRP bars due to severe exposures as in an infrastructure environment; thus, the corresponding enhancement methodologies and service life predictions of infrastructure containing BFRP bars have been established. Wu et al. [14] have adopted an Epoxy-Based BFRP exposure experimental program to study the local and global degradation due to harsh environmental conditions. Epoxy-based BFRP bars were exposed to different environments as alkaline, saline, acidic and water as a simulation of the natural conditions of civil infrastructure environments. The testing was executed under certain temperature changes (22 and 55ºC) as an accelerating agent. The exposure periods were set to 7, 18, 34, and 66 days. The experimental program included the conditioning of glass and carbon composite bars at a temperature of 55ºC for a 66-day duration for the sake of comparative analysis. The matrix degradation played a big role in the durability

behavior of FRP bars; however, its influence was studied closely on the global deterioration of the composite. Furthermore, the degradation program included fiber, matrix, and composite levels. The test results generally showed that the BFRP were most affected by alkaline and acidic exposures, while no major corrosion took place in saline or water environments. Moreover, the elastic modulus of BFRP bars has not experienced any changes, and the BFRP bars exhibited a fair performance in terms of corrosion resistance while exposed to extreme conditions compared to previously used bars. This phenomenon was the result of the resin bonding and matrix protection involved; hence, the degradation is limited. Degradation in water and saline water were represented by local etching, while during the alkaline exposure, large pitting occurred causing a large loss in the tensile strength of the bars. The acidic solutions changed the chemical composition of the fabric matrix, which lead to a loss in tensile strength retention. Mainly, BFRP exhibited less acidic corrosion than GFRP bars. Finally, the CFRP bars showed better corrosive resistance in all kinds of harsh environments than the BFRP bars.

Chen et al. [19] used the Arrhenius relation in long-term behavior prediction for GFRP, based on short-term accelerated aging tests data. The GFRP bars were exposed to simulated concrete solutions at different temperatures, where the durability performance was measured based on the tensile strength before and after exposure. A modified Arrhenius analysis was conducted to evaluate the validity of accelerated aging tests. Sustained loads were applied while the exposure was taking place.

Serbescu et al. [34] have conditioned and tested 132 spiral-ribbed BFRP of two types (epoxy and vinylester resins) and seven different diameters (3, 4, 5, 6, 7, 8, and 10 mm). The conditioning solutions varied in pH (pH 7, pH 9, and pH 13), and the temperatures of conditioning were 20, 40, 60ºC for four exposure periods; 100, 200, 1000, 5000 hours. A predictive model was established to determine the future design tensile strength of the BFRP. The experimental program was discussed briefly in the paper; however, the main concern was to utilize the tests results to modify the model fib Bulletin 40 (2007) for long-term prediction of the mechanical properties of BFRP exposed to different environments. Therefore, the BFRP specimens were tested for tension and elastic modulus after they were exposed to different pH level solutions, at different temperatures, and for various durations of exposure. Three sets of tensile

strength testing were implemented, each set targeted bars with different diameters and exposure conditions. All specimens were tested till failure, in which the failure was preceded by splintering as a warning. As a result, the tensile strength of the BFRP bars ranged from 972 to 1481 MPa with a maximum Young's modulus of elasticity of 47 GPa. Moreover, it was found that the temperature is the most governing factor in terms of degradation; for instance, the specimens exposed to the 9-pH solution at 60ºC for 5000 h experienced around 69% of tensile strength retention. Therefore, increasing the pH levels increases the strength loss (around 8% additional loss), where the elastic modulus exhibited some sort of increment due to the curing of the matrix while conditioning. A degradation prediction model was established, which is capable of predicting the long-term strength of BFRP bars exposed to any given environment.

In a recent study [24], two types of ribbed GFRP bars (8 and 9 mm outer diameters) were studied under severe and accelerated aging conditions; mainly, targeting the mechanical properties and the degradation performance before and after the conditioning. The tensile behavior and the modulus of elasticity were determined after exposing the samples to severe exposures and sustained loading for certain exposure periods. This study provided statistical visuals which support the comparative characterization. The experimental program encompassed the testing of 42 GFRP samples, where 6 samples were kept as control samples without conditioning and the rest of the samples were exposed to accelerated aging conditioning. The samples were exposed to seawater-contaminated concrete for different durations of conditioning; 150, 300, 450 days. The ambient temperature in the temperature-controlled tanks was set to be 20, 40, 60 °C. For each testing condition, 3 trials were performed. The test specimens were 1200 mm long, the middle third was cover with the concrete (50x50 mm cross-sectional shape). Ordinary Portland cement concrete was used with 1:1, crushed sand-to-dune sand ratio, and maximum aggregate size of 10 mm. The parts that were exposed to tap water directly were covered by PVC pipes to seal them from conditioning. The testing program included uniaxial tensile testing till failure for the conditioned bars after they were taken out carefully from the concrete. The PVC pipes were removed to allow the installation of the steel end grips with the proper amount of epoxy to maintain enough bonding while the test runs. Three deflection gages were installed, in the middle, and 100 mm from the endpoints. As a result, the tests showed that GFRP

experienced a loss in the tensile retention which is directly proportional to the duration of exposure to simulated sea-water-contaminated concrete. Also, it was observed that the higher initial tensile strength of the bar, the higher the loss in tensile retention. Sometimes, once the moisture absorption reaches an equilibrium state, the release of residual stresses caused some kind of recovery improving the tensile behavior. The temperature resulted in a further degradation of the tensile strength in different moisture conditions.

Another very recent study was conducted on GFRP in water-contaminated concrete to evaluate the durability performance and characterize it micro-structurally by El-Hassan et al. [35]. Two types of commercially produced GFRP bars were studied by exposing them to seawater-contaminated concrete immersed in tap water. The exposure periods included 5, 10, 15 months at temperatures of 20, 40, and 60 °C. The control specimens testing included uniaxial tensile testing, and a set of testing procedures were conducted for microstructural analysis such as: differential scanning calorimetry (DSC), scanning electron microscopy (SEM), Fourier transform infrared (FTIR) spectrometry, and matrix digestion using nitric acid. GFRP type I had an inner and outer diameter of 7.2, and 8 mm respectively, while type II had 8, and 9 mm of those. The results have proved that the GFRP bars with the higher moisture uptake exhibited higher strength reductions (type II), where type II had a lower matrix retention after conditioning. Both types of GFRP featured a lower glass transition temperature because of the harsh exposure. It was shown that the temperature factor was dominant as a degradation factor rather than the duration factor, in other words, the GFRP degradation was more affected by the temperature impact.

2.2. Surrounding Media

The surrounding media is one of the most significant parameters that influence the durability of FRP composites. The surrounding environments or media includes water, alkaline solution, acidic solution, and saline solution. The degradation effect is governed by the chemical properties and the concentration of the surrounding solution.

Fang et. al [37] studied the effect of water plasticization on the unconditioned GFRP specimens, thereby reducing the T_g value from 78.5^{o}C to approximately 76.2^{o}C

after conditioning. The GFRP, due to water and seawater six-month exposure, exhibited a major drop in the tensile strength value results.

Moreover, Davalos et al. [38] has concluded that the natural saturated concrete environment affects the GFRP specimens more aggressively than open air environment, however, the bars exhibited a tensile loss of around 13% after 150 days of saturated concrete conditioning at 20^{o}C. While the GFRP bars experienced 1% tensile loss in open air environment.

Chen et al. [19] has observed that the harshest attack was the alkaline solution attack represented by leaching, embrittlement, and etching of the GFRP fibers. The matrix protection was exhausted because of the hydrolysis and swelling leading to major degradation failures and tensile retention loss.

Similarly, Li et al. [39] indicated, the degradation of matrix resin of BFRP bars at 60^{o}C temperature, conditioned in alkaline solution was more significant than the degradation in the water immersion.

Alkaline solution exposure simulates the concrete alkalinity that attacks reinforcing bars. Alkaline chemical reaction with the fibers leads to mass and tensile strength losses. It is worth mentioning that Resin plays an important role protecting the integrity of FRP composites [40]. Vinylester showed a remarkable performance regarding alkaline attack resistance in GFRP bars [7]. The chemical stability of BFRP bars will be investigated in this study by exposing the bars to the alkaline solution. The extent of alkaline effect can be measured by the mass loss and tensile strength retention [41]. Alkaline solution impregnates into the BFRP resin causing swelling and into the fiber-resin interface causing major changes in the mechanical properties of BFRP bars.

2.3. Temperature Factor

Temperature is considered as a major accelerating factor in durability studies. The higher the temperature, the greater and the quicker the damage occurs to FRP composites. Based on Wang et al's [36] studies, ambient temperatures of 32, 40, 48, and 55^{o}C lead to tensile retentions of 92.7%, 81.7%, 59.1% and 26.0% respectively, BFRP bars conditioned in moist normal seawater sea-sand concrete (N-SWSSC) for

63 days. Ambient temperatures of 32, 40, and 55^{o}C lead to tensile retentions of 97.9%, 90.2% and 77.4%, respectively, BFRP bars conditioned in moist high performance seawater sea-sand concrete (HP-SWSSC) for 63 days. Ambient temperatures of 32, 40, and 55^{o}C lead to tensile retentions of 87.4%, 90.8% and 80.1%, respectively, GFRP bars conditioned in moist normal seawater sea-sand concrete (N-SWSSC) for 63 days. Ambient temperatures of 32, 40, and 55^{o}C lead to tensile retentions of 97.9%, 94.1% and 89.6%, respectively. GFRP bars conditioned in moist high performance seawater sea-sand concrete (HP-SWSSC) for 63 days.

Gang et al. [14] reported that the tensile retention was reduced from 99.1% to 82.0% when the temperature was 25**^{o}C** and 55^{o}C respectively. However, the results showed the big role that the temperature plays in increasing the rate of degradation.

Another recent study focused on tensile retention of loaded concrete-encased GFRP specimens, it turned out that the tensile retention was 97% and 87% when the ambient controlled temperatures were 20 and 60^{o}C, respectively, for a 30-day duration. The temperature accelerating effect was more distinct in the greater exposure rotation (210 days). Similarly, the tensile retention of loaded concrete-encased GFRP specimens was 80% and 49% when the ambient controlled temperatures were 20 and 60^{o}C, respectively. The sustained load reduced the tensile retention by around 3% in 20^{o}C temperature, while no effect was recorded when the temperature was 40^{o}C or 60^{o}C [38].

Based on Robert et al.'s [20] research experimental data, tensile losses of 16%, 10%, and 9% were noted after 230 days of exposure duration in tap water at 50, 40 and 23^{o}C temperatures. The higher temperatures cause a greater rate of water diffusion into the fiber matrix quickening the degradation and swelling process of the fiber-matrix interface, as a result, the overall tensile strength will be lowered.

A durability study reported water uptake percentages of 0.1, 0.26, 0.32, and 0.56% of the 6-month conditioning at 20, 40, 60, and 80^{o}C in distilled water, while they were 0.14%, 0.20%, 0.47% and 0.63% of the 6-month conditioning at 20, 40, 60, and 80^{o}C in distilled water. However, there is a directly proportional relationship between water uptake and conditioning temperature in the experimental results [32].

2.4. Time of Exposure Factor

As a general rule, the time of exposure governs the degradation extent in any durability study. A recent durability study emphasized that regardless the type of ambient environment, temperature, or sustained load level, the time of exposure has an influence on the tensile loss of FRP composites. The tensile losses were recorded to be 9.7%, and 15% when the FRP bars are subjected to 40^{o}C-Alkaline environment for a duration of 21 and 63 days respectively [14].

Robert and Benmokrane [42] indicated that the temperature factor is more influential as a durability factor than the time of exposure. Moreover, the tensile retention of GFRP bars conditioned for 60 days at 23^{o}C was 99% while it was 94.8% after they were conditioned for 240 days in the same environment.

Based on the literature review stated above, it can be observed that there is a gap regarding the durability of BFRP under harsh temperature-accelerated environments, focusing on the natural concrete environment and compared to alkaline environment. The research study targets to fill the gap in our knowledge in this area.

In this research, the durability of Basalt Fiber Reinforced Polymers (BFRP) bars of 10 mm diameter is studied after direct exposure to severe conditions. The main aim is to investigate the degradation performance of the microstructure and tensile properties of these BFRP bars under accelerated conditionings that simulate the concrete environment. A set of BFRP bars is wrapped by concrete prisms and immersed in tap water. Another set of BFRP bars is exposed to alkaline solution. In concrete-wrapped and alkaline exposures, temperatures of 20^{o}C, 40^{o}C, 60^{o}C are maintained in isolated tanks for durations of 2880 h, 5760 h, and 8760 h. To achieve the main goals of this project, the experimental program will include Un00iaxial Tensile Tests, S^{c}anning Electron Microscopy (SEM), Water Absorption, Differential Scanning Calorimetry Analysis (DSC), Fourier Transform Infrared Spectrometry (FTIR), Matrix Digestion, and Fiber Volume Fraction Analysis.

Chapter 3. Experimental Program

This section provides a full description of materials used in the research, types of exposures, and testing program in order to accomplish the previously mentioned research objectives. The test matrix was divided into two groups, mainly; a group of BFRP bars that will be conditioned with and without concrete encasement and a group of segmented BFRP bars that will also be conditioned for microstructural purposes. The testing program was conducted before and after conditioning to study the durability performance and microstructures, which includes Scanning Electron Micrographs (SEM), Water Absorption, Differential Scanning Calorimetry Analysis (DSC), Fourier Transform Infrared (FTIR) Spectrometry, Matrix Digestion, and Fiber Volume Fraction Analysis.

3.1. Test Program

The experimental matrix was developed based on the exposure type and the specimens were divided as per following two groups, with exposure durations of 3, 6, and 9 months:

- Group 1: Alkaline exposure + Temperature 20^{o}C, 40^{o}C, and 60^{o}C

- Group 2: Concrete-encased bars + tap water immersion exposure + Temperature 20^{o}C, 40^{o}C, and 60^{o}C

Three replicated samples were considered for each testing criterion. Table 3-2 illustrates the test matrix, where three replicate samples were taken as control samples, twenty-seven BFRP specimens were conditioned in temperature-accelerated alkaline environment, twenty-seven concrete-encased BFRP bars were conditioned in temperature-accelerated alkaline environment. Additionally, eighteen concrete-encased small BFRP bars were subjected to temperature-accelerated alkaline and tap water environments. Durations of 3, 6, and 9 months were set as exposure periods.

Table 3-3 illustrates the test matrix of microstructural testing program. Solid cut pieces samples (1 cm-thick) were prepared for moisture uptake, SEM, and matrix digestion. While powder samples (5-10 mg) were produced from the conditioned and the unconditioned bars for DSC and FTIR tests. The testing program was selected based

on comparison criteria, accelerating factors study and comparison, and the need to verify the tensile testing of the bars. The nine months exposure period was taken into consideration for all temperatures and environments in order to examine the most extreme conditions of each and every type of environment. This will grant the ability to study the temperature effect as an accelerating factor. All exposure periods of the 40^{o}C conditioning were considered to conduct an extensive comparison between the types of environments and to take a closer look at the influence of each type of conditioning on the durability, chemical resistance, and physical endurance of the BFRP bars.

3.2. Materials

3.2.1. Concrete prisms: properties and mix design. Ordinary Portland cement concrete mix possessing a compressive strength of 40 MPa was utilized in this research as a coating to cover the middle third (30 cm portion to be encased) of the BFRP bars, and immersed in tap water. In addition to Ordinary Portland cement (ASTM Type I), a maximum aggregate size of 10 mm and dune sand are used in this mix. Table 3-4 illustrates the concrete mix constituents and their proportions as a unit weight (kg/m^3) that were used in this study. In order to optimize the workability without reaching an increased water/cement ratio, Superplasticizer of a type PCE-270 was applied. The concrete slump value was 180±30 mm.

3.2.2. BFRP bars. In this research, sand-coated BFRP bars with diameters of 10 mm were considered. The properties of each bar size including the cross-sectional area, ultimate tensile strength, ultimate strain, and elastic modulus are first determined as a benchmark prior to the conditionings program. The average cross-sectional area of BFRP bars are computed according to the method specified by the ACI 440.3R-12 [1]. The test method is conducted by immersing a BFRP cut piece in tap water, then removing it. Afterwards, the difference between the two volumes, before and after immersing the BFRP cut piece, was utilized to obtain the cross-sectional area [1]. Accordingly, the average cross-sectional area of the bar was found to be 94.3 mm. Since there is only one type of surface treatment for each BFRP bar, the designation will not include the surface treatment type. The sand-coated bars have shallow patterns of indentations spaced by 3mm spaces along the bar, providing a uniform texture. The

sand coating surface helps increase the friction with concrete and the overall bond strength.

Table 3-2: Test matrix

BFRP Diameter (mm)	Surrounding media	Temperature (°C)	Time of Exposure (Months)	# of Samples for Tensile Testing	# of Samples Microstructural Tests
10	Control			3	1
	G1: Alkaline	20	3	3	1
			6	3	1
			9	3	1
		40	3	3	1
			6	3	1
			9	3	1
		60	3	3	1
			6	3	1
			9	3	1
	G2: Moist Encased-concrete bars	20	3	3	1
			6	3	1
			9	3	1
		40	3	3	1
			6	3	1
			9	3	1
		60	3	3	1
			6	3	1
			9	3	1
				57	**19**

Table 3-3: Microstructural test program

BFRP Group	Temperature (°C)	Time of Exposure (Months)	SEM	Moisture Uptake	Matrix digestion analysis	FTIR	DSC
Control			✓	✓	✓	✓	✓
G1: Alkaline	20	3					
		6					
		9	✓	✓	✓	✓	✓
	40	3	✓	✓	✓	✓	✓
		6	✓	✓	✓	✓	✓
		9	✓	✓	✓	✓	✓
	60	3					
		6					
		9	✓	✓	✓	✓	✓
G2: Moist Encased-concrete bars	20	3					
		6					
		9	✓	✓	✓	✓	✓
	40	3	✓	✓	✓	✓	✓
		6	✓	✓	✓	✓	✓
		9	✓	✓	✓	✓	✓
	60	3					
		6					
		9	✓	✓	✓	✓	✓

Table 3-4: Concrete mix proportions

Concrete mix constituents	unit weight (kg/m3)
OPC	370
Water	171
10-mm aggregate	907
5-mm Washed aggregate	343
5-mm Crushed aggregate	318
Dune sand	329
PCE-270	6.6
w/c	0.41

Several tests were conducted on BFRP bars such as Glass Transition Temperature by DSC Analysis (T_g), Fiber volume fraction, fiber content ratio % by weight, the average cure ratios and transverse coefficients of thermal expansion.

The void contents of BFRP bars were determined as 0.24% as per D2734-16 and ASTM D3171 [39]. The mass fraction of BFRP by matrix digestion using nitric acid, in accordance with ASTM D3171, was 74.5%. The as received tensile strength and modulus, determined conferring to the test method Identified by the ACI 440.3R-12 [1], were 1268±15 MPa and 48±3 GPa.

3.2.3. Conditioning tanks. Three fiber-glass and temperature-controlled tanks were prepared at the United Arab Emirates University as shown in Figure 3-2 to include the test specimens in water conditioning. Two of them are equipped with built-in heaters and thermostat in order to monitor a maintained temperature accurately. Temperatures of 20^{o}C, 40^{o}C, and 60^{o}C were considered in this research during the exposure periods. The BFRP bars ends were covered and sealed by Polyvinyl Chloride pipes (PVC) before immersion, hence, these regions are protected from the harsh exposure.

Figure 3-2: Temperature-controlled conditioning tanks

The PVC tubes were replaced by steel tubes after conditioning for tensile testing. Results of exposed specimens were compared with the control unexposed specimens that have been tested already.

Three stainless steel-made and temperature-controlled tanks were prepared at the United Arab Emirates University, as shown in Figure 3-3, to include the test specimens in alkaline conditioning. Two of them are equipped with built-in heaters and thermostat in order to monitor a maintained temperature accurately.

Figure 3-3: Stainless Steel tanks for alkaline conditioning

3.2.4. Alkaline solution. In order to prepare an alkaline solution that possesses the internal void water pH of concrete, 40 g/L of NaOH to be added and mixed properly with water, the alkaline solution PH obtained using Laqua pH-meter probe was 11.45 as shown in Figure 3-4.

Figure 3-4: Laqua pH-meter reading for the alkaline solution

3.3. Fabrication and Test Specimens

The concrete was cast in wooden molds to produce 50×50×300 mm prisms that cover the middle portion (30 cm portions) of the 10 mm-diameter bars, as shown in

Figure 3-5. However, the 50×50×200 mm prisms were cast for microstructural tests as shown in Figure 3-6. Once the prisms were hardened, they were wrapped by cloths and sprayed by potable drinkable water for 28 days to be cured properly, then removed to natural environment till the exposure tanks are ready for running the conditioning. The previously mentioned stages are illustrated in Figure 3-7. Compressive strength, splitting strength, and ultrasonic pulse velocity tests were conducted (according to ASTM C39, C496, and C597) [44, 45, 47].

Figure 3-5: Typical 10-diameter concrete-wrapped bars detailing

Figure 3-6: Typical microstructural specimens detailing

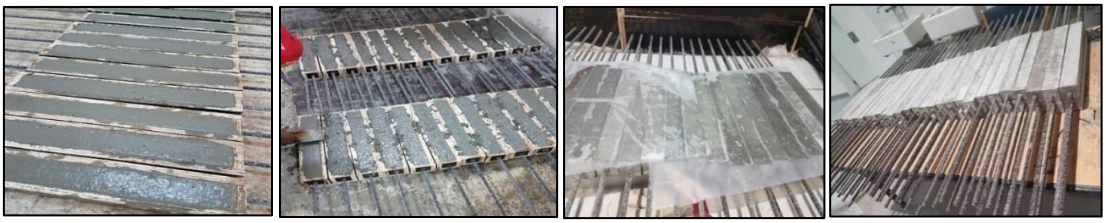

Figure 3-7: Concrete prisms casting and curing

Figure 3-8: Microstructural concrete-wrapped prisms

3.3.1. Moist concrete-encased specimens. Twenty-seven BFRP specimens were considered for tensile testing (300 mm long concrete prisms), the middle 300 mm-portion was encased by concrete to represent the actual field condition. The uncoated BFRP portions were covered by PVC (Polyvinyl Chloride) pipes at the ends by silicone to eliminate water leakage into the PVC pipe as shown in Figure 3-9. Nine concrete-encased specimens (200 mm long concrete prisms, as illustrated in Figure 3-8) were considered for microstructural tests. Figures 3-10a and 3-10b show schematic drawings detailing of the concrete-wrapped BFRP specimens detailing.

Figure 3-9: Concrete-wrapped specimens

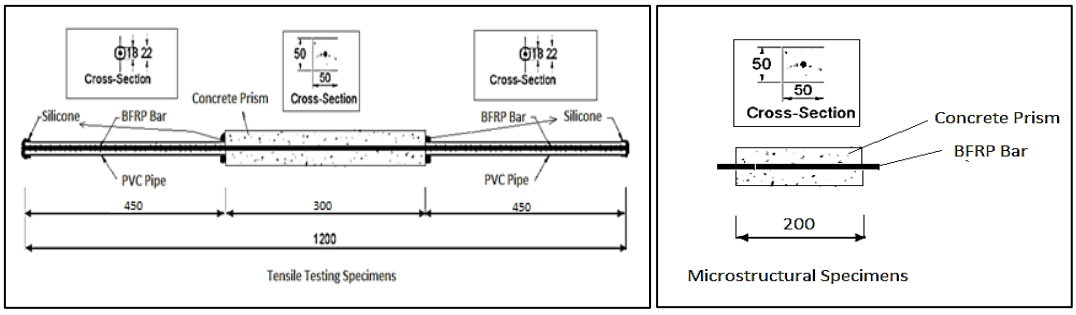

(a) (b)

Figure 3-10: Concrete-wrapped specimens detailing (in mm)

The PVC pipes provided the protection for the exposed portions from the ambient harsh conditioning. The tanks were equipped with built-in heaters and thermostat, thereby emitting temperatures of 20, 40 and 60^{o}C on the specimens. After the conditioning, the concrete was removed gently and the PVC tubes were replaced by steel-end-grips for tensile testing.

3.3.2. End grips. Concrete-wrapped Specimens end grips were 450 mm-long steel tubes, shown in Figure 3-11, with an inner and outer diameter of 32.4 mm and 40 mm respectively. The inner surface was cleaned carefully with corrosion removal

chemical and roughened before installation, where the steel tubes were painted for pleasant appearance and proofing. The adhesive grouting material used to provide enough bond between the BFRP and the grip was Nano-Grout Pourable produced by Conmix LLC, as shown in Figure 3-12. It consisted of two parts: part A (base) and part B (hardener), The ratio of mixing the base with the hardener is 2:1. The BFRP bars were centered using Teflon rings (Figure 3-11), fabricated to allow the bar to be stable and centered. The exterior end Teflon caps were solid in the last 1cm to eliminate any grout leakage.

Figure 3-11: Steel grips and teflon rings

Figure 3-12: Nano-grout used as a bonding material between the bar and the end-grip

3.4. Properties of Surrounding Concrete

3.4.1. pH value. pH stands for the concentration of hydrogen ions, where the pH ranges from 1 to 14. Any solution that possesses a pH below 7 is considered as acid, pH of 7 is neutral, and pH greater than 7 is basic. Concrete was crushed into powder of 5 g and mixed with 10 mL fresh distilled water (pH=7) properly. The pH meter was calibrated and used to determine the pH of mixture. As a result, the pH was found to be 12.45 which is, according to ASTM E70-07 [46], considered as an alkaline surrounding environment.

3.4.2. Compressive strength test. The compressive of the concrete strength was determined using a compression machine with 3000 kN capacity, as shown in Figure 3-13. The testing was conducted in the Construction Materials Laboratory at AUS. The testing method complies with ASTM C39/C39M-17A [47]. Three standard cylinders and three standard cubes were tested as shown in Figure 3-14, and the average compressive strength was around 46.6 MPa.

Figure 3-13: Automated compressive strength machine

Figure 3-14: Compressive strength testing

3.4.3. Splitting tensile strength test. Splitting tensile strength is a very crucial parameter that indicates the structural integrity level of concrete. Splitting tensile strength was conducted on 3 (as shown in Figure 3-15) standard cylinders in the Construction Materials Laboratory – American University of Sharjah according to ASTM C496/C496M-11 [45]. The splitting tensile strength was found to be 3.22 MPa.

Figure 3-15: Splitting tensile test

3.4.4. Ultrasonic pulse velocity test (UPV). This test enables the researcher to evaluate the structural integrity of concrete. It indicates any voids or cracks existing in the concrete. As shown in Figure 3-16, the UPV consists of velocity meter, transmitter, receiver, and lubricant. The test method complies with the direct method specified in ASTM C597-16 [44] using PROCEQ Instrument. By measuring the distance (height of cylinder) in meters and velocity of wave in (μs), we can find out the time elapsed for the wave to cross from the transmitter to the receiver. This reading indicates the quality, homogeneity, and density of concrete.

Figure 3-16: UPV equipment

The average UPV reading obtained was 4.69 km/s. From Table 3-5, the quality of concrete is said to be an excellent quality.

Table 3-5: Concrete quality based on UPV value [43]

Paulse Velocity (km/s)	Quality of Concrete
>4.5	Excellent
3.5-4.5	Good
3.0-3.5	Medium
<3.0	Doubtful

3.5. Properties of BFRP Bars

3.5.1. Moisture absorption. Water absorption test enables the researcher to study the FRP composite water absorption portability as shown in Figure 3-17. Recent studies showed that the water intake by FRP composite in room temperature is linear in the beginning and increasing till it reaches a saturation point [6]. The water absorption test conducted in this study complies with ASTM D570 [48]. The saturation absorption is accomplished after a prolonged time; however, this designates the time dependency in water absorption of FRP [49]. The temperature is considered as a major accelerating factor of water ingress, the higher the temperature leads to a higher rate of water ingress and weight of absorbed water. The test delivers the net weight gain of water as a percentage of the overall specimen weight. The water ingress into the fiber-resin interface may cause losses in tensile strength but an improvement in cyclic loading performance [32]. The Moisture uptake can be determined using the following formula (3.1):

$$Moisture\ uptake\% = \frac{100x(Conditioned\ mass - Oven-dried\ mass)}{Initial\ mass} \quad (3.1)$$

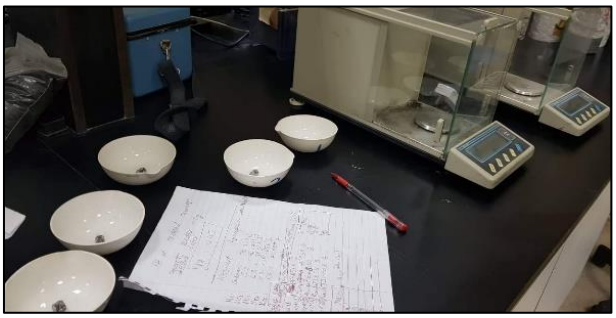

Figure 3-17: Moisture absorption procedure

3.5.2. Scanning electron microscope (SEM). The scanning electron microscope provides high-quality images which characterizes the damage induced by harsh environments in the bars. The SEM (Model JEOL-JSM 6390A) is composed of

three main detectors as shown in Figure 3-18, mainly: Energy Dispersive Spectrometer (EDS), Back Scattered Electron Detector (BSE), and Secondary Electron Detector (SE). The main concept of the SEM is that the electrons interact with the material surface atoms generating various wavelengths that reflect the sample surface topography and compositions. The micro crack density can be obtained by using (imageJ) software that detects the contrast variations between pixels. In order to produce a good-quality image as demonstrated, the contrast between the micro crack and surface has to be adjusted properly, the higher degree of contrast the more distinct the cracks will appear. It is worth mentioning that the surface to be tested has to be flat and polished using a grinder polish machine. A cut through the exposed sample is required to obtain a clear image, however, the cut should not compress or erase the cracks or pits by using highly sensitive cutting equipment. To enhance the quality of reflected electron image, the sample was cut using diamond saw, gold coated with a thin gold layer as shown in Figure 3-19. The best cutting results are obtained by using a micro-cutting machine which provides an automatic precision and easy cutting speed control [49].

Figure 3-18: JEOL-JSM 6390A Scanning electron microscope

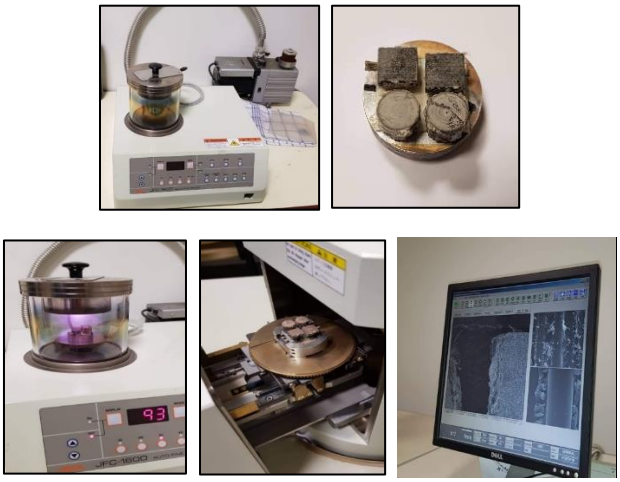

Figure 3-19: Gold coating and test procedure

3.5.3. Matrix digestion using nitric acid. Matrix digestion enables obtaining the percentages of matrix and fibers. It's conducted by mixing 0.5-1.5 g of BFRP powder with 50 mL of 70% aqueous nitric solution according to ASTM D3171 [43]. The mixture is then exposed to 80^{o}C temperature for 6 hours. However, the chemical reaction which takes place between the BFRP and nitric acid causes the dissolution of epoxy resin. Furthermore, the fibers remain uninfluenced in which the remaining mass was washed with distilled water and oven-dried for 1 hour at 100^{o}C. The following equation (3.2) expresses the matrix content.

$$Matrix\ Content\ (\%, mass) = 100\ X\ Initial\ mass - Final\ mass\ initial\ mass \quad (3.2)$$

3.5.4. Differential scanning calorimetry (DSC). The differential scanning calorimetry analysis is a thermo-analytical technique which measures the heat required to change the temperature of a sample with respect to a reference as a function of temperature. The test is conducted in accordance with ASTM D3418 [51]. Glass temperature is considered as a specific heat step change. This parameter indicates important information about the chemical, mechanical, and electrical behavior. It also leads to the thermal history, and conditioning processing [52]. The analysis is implemented for materials which possess distinct heat capacity. The DSC analysis produces DSC curve (Temperature or Time vs. Heat flow) of a material. The test delivers a very important parameter of a polymer generally or an FRP composite specifically, the glass transition temperature ($\boldsymbol{T_g}$). It is defined as the temperature where a polymer transforms from hard state to melting or rubbery state [53]. Figure 3-20 illustrates the DSC apparatus and procedures conducted.

Figure 3-20: DSC apparatus and testing procedures

3.5.5. Fourier transform infrared spectrometer (FTIR). The Fourier transform infrared spectrometry is a technique in which the infrared spectrum of the

absorption or emission of a solid can be obtained. The test is conducted using an FTIR spectrometer which is able to receive a high resolution of a wide range of spectral Data [53]. The hydrolysis reaction of a sample is studied through this test indicating the degradation behavior over the conditioning duration. A sample of 100 mm length is powdered by potassium bromide (KBr = 1:4 by mass). The mixed powder then tested using a Varian 3100 FT-IR spectrometer at United Arab Emirates University [35].

3.5.6. Tensile strength testing. Uniaxial tensile tests are conducted on a total of 3 unconditioned control specimens, and 54 conditioned specimens to measure the ultimate stress and modulus of elasticity using a Universal Testing Machine (UTM) available at the American University of Sharjah. Three replicas of each type of exposure and temperature were equipped with end-grips installed using nano-grout. Transducers were installed (as illustrated in Figure 3-21) in the middle of the gauge length which enables to accurately determine the strain and hence the modulus of elasticity of the bar. To support the transducer data, three strain gauges were installed at 1/3 of the gauge length on both sides and at the mid-point.

Figure 3-21: Tensile testing setup

The testing region is the middle 300 mm. The grips were 450 mm long as shown in the schematic (Figure 3-22). The ultimate tensile strength was determined as well as the moduli of elasticity from the stress-strain diagrams generated.

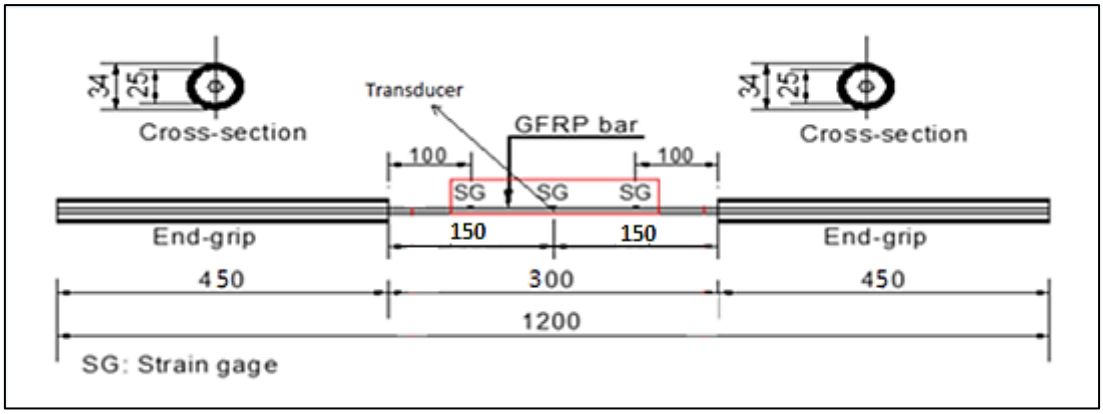

Figure 3-22: Tensile setup schematic

The modulus of elasticity was calculated by computing the slope of the stress-strain curves according to Equation 6.3 in accordance to ACI 440.3R-12 [1]:

$$E_f = \frac{f_{50} - f_{20}}{\varepsilon_{50} - \varepsilon_{20}} \tag{3.3}$$

where:

f_{50} : is the stress at 50% of the tensile strength,

f_{20} : is the stress at 20% of the tensile strength

ε_{50}: is the strain at 50% of the tensile strength

ε_{20}: is the strain at 20% of the tensile strength.

Chapter 4. Results and Discussion

This section of the report will provide a summary of results for the tests that have been conducted along with a brief discussion. Results and comparisons of moisture absorption, tensile strength loss, modulus of elasticity, failure mode, matrix digestion, FTIR and DSC will be presented, analyzed, and discussed in this chapter.

4.1. Moisture Uptake

Due to the continuous conditioning in aqueous solutions, the water or alkaline molecules penetrate the FRP composite by diffusion through the surface micro-cracks and then transfer through the matrix chains and capillaries. Table 4-6 states the moisture uptake percentages for the conditioned samples which were represented in Figures 4-23 and 4-24. The specimen is designated by the exposure period followed by the type of conditioning and the ambient conditioning temperature (e.g. 3A20 stands for specimens conditioned in alkaline exposure for 3 months at 20^{o}C). U group stands for the moist concrete-wrapped bars. Figure 4-23 shows the exposure period effects, as the duration of conditioning increases, the aqueous molecules continues to penetrate and diffuse through the cracks, and gaps been propagated. Figure 4-24 represents the temperature effect, as the temperature increases, it accelerates the molecules more often to penetrate and impregnate into the micro-cracks. Alkaline group conditioned at 20^{o}C for 9 months moisture uptake can be estimated as 0.68%. However, the temperature as an accelerating factor increased the rate of diffusion into the FRP matrix capillaries. The moisture uptake will pursue increasing until the BFRP reaches an equilibrium state of saturation. The greatest moisture uptake achieved in alkaline and moist concrete-wrapped groups were 1.04% and 0.68% respectively. 3-months conditioning at 40^{o}C had a negligible effect on the moisture uptake of both groups.

Regarding the conditioning regime, as noticed from the Figures below (4-23 and 4-24), alkaline group exhibited greater moisture uptake percentages as they are exposed directly to the aqueous solution unlike the concrete-wrapped specimens groups which are encased by a concrete cover of 2 cm over the perimeter of the bar. This higher moisture uptake of alkaline group is due to the greater progression of matrix softening and impairment of fiber-matrix interface bonds.

El-Hassan et al. [35] indicated that, with the increase of temperature and exposure period, the moisture uptake increases. However, this relationship was confirmed in this research as discussed above. The highest percentage of moisture uptake recorded in El-Hassan et al.'s research was found to be around 1.5% for GFRP bars wrapped by seawater-contaminated concrete and immersed in tap water for 15 months at 60°C. Based on El-Hassan et al.'s results, the moisture uptake increased within the first 10 months more rapidly than it did at later stages. In this study, it's observed from Figure 4-23 that the behavior of moisture uptake tends to reach a constant value in greater exposure period. Another recent study by Benmokrane et al. [31] focused on the moisture uptake of epoxy-based BFRP and vinylester-based GFRP bars conditioned for 5,000 hours in alkaline solution at 60°C. The two types exhibited different moisture uptake percentages of 0.26% and 0.79% for vinylester-based GFRP, and epoxy-based BFRP respectively, where the corresponding moisture uptake percentages of control ones were 0.21% and 0.47% respectively.

Table 4-6: Moisture uptake for conditioned specimens

Duration Effect	
Sample	Moisture Uptake%
Control	0
3A40	0.22
6A40	0.67
9A40	0.94
3U40	0.12
6U40	0.34
9U40	0.41
Temperature Effect	
Sample	Moisture Uptake%
Control	0
9A20	0.19
9A40	0.94
9A60	1.04
9U20	0.68
9U40	0.41
9U60	0.66

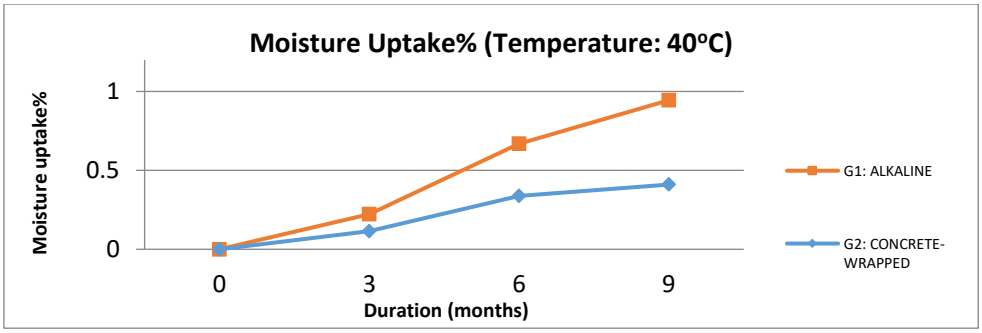

Figure 4-23: Moisture uptake (Duration)

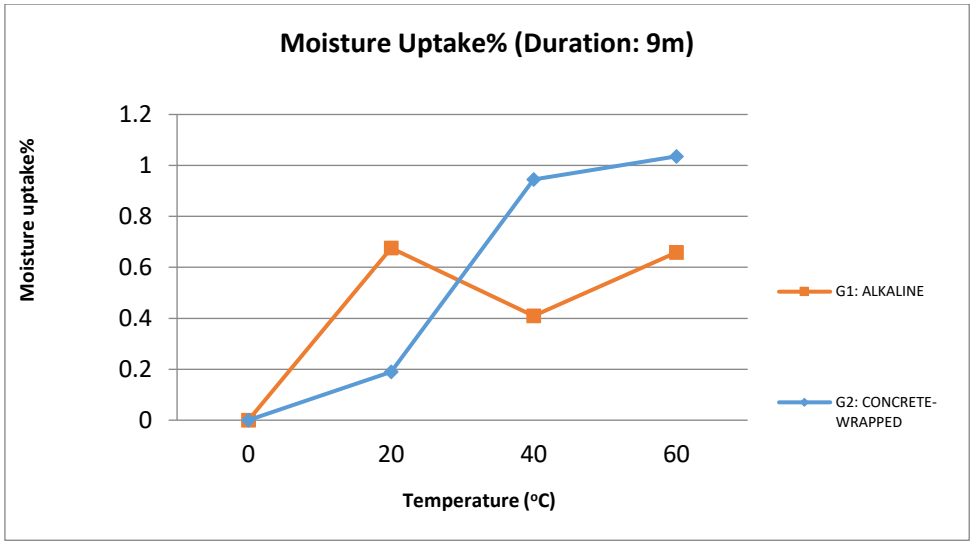

Figure 4-24: Moisture uptake (Temperature)

4.2. Tensile Mechanical Performance

4.2.1. Tensile strength. The BFRP exhibited a linear elastic stress-strain response up to the detachment of fibers and eventually failure. The linear elastic response is due to the constant increment of tensile stressing of 3 mm/s rate. However, when it reaches to the maximum tensile capacity (peak), the fibers start to detach and the resin to crumble. The modulus of elasticity is determined by calculating the initial slope of stress-stain response of the bar. Table 4-7 states ultimate load capacity, ultimate tensile strength, and tensile modulus of elasticity for the control and conditioned BFRP samples. Table 4-7 results are represented later in this section in bar charts (Figures 4-25 to 4-29), in order to compare the different categories of data.

Tensile strength results of BFRP bars, conditioned in an alkaline environment and moist concrete-encased, are shown in Figures 4-25, 4-26, and 4-27. For the case of alkaline environment, three-month conditioned samples exhibited insignificant tensile strength reductions of 4, 3, and 8% at 20, 40, and 60°C, respectively. Some six-month conditioned samples also exhibited relatively higher tensile strength reductions of 5, and 17% at 40, and 60°C, respectively, while the samples subjected to 20°C exhibited a negligible reduction in tensile strength. Nine-month conditioned samples exhibited much greater tensile strength reduction of 4, 13, and 29% at 20, 40, and 60°C, respectively. While the samples subjected to 20°C exhibited a negligible reduction in tensile strength of 4%. This tensile strength reduction is caused by the effect of alkaline

Table 4-7: BFRP control and conditioned specimens mechanical properties

Specimen	Ult. Load (kN)	Ult. Tensile Strength (MPa)	E (GPa)
Control BFRP	119.64	1268.31	47.16
3A20	114.48	1213.59	41.00
3A40	116.57	1235.79	41.05
3A60	109.50	1160.80	46.72
3U20	112.92	1197.04	49.90
3U40	111.92	1186.51	56.25
3U60	105.31	1116.36	44.57
6A20	117.55	1246.16	38.63
6A40	113.65	1204.85	46.36
6A60	99.31	1052.74	56.33
6U20	112.24	1189.86	50.11
6U40	107.91	1143.91	49.05
6U60	105.80	1121.57	43.00
9A20	114.66	1215.52	48.13
9A40	104.30	1105.69	46.57
9A60	85.53	906.68	45.60
9U20	108.54	1150.68	48.97
9U40	108.16	1146.58	49.95
9U60	101.80	1079.18	46.75

solution, weakening and disintegrating the chemical bonds at the fiber-matrix interface, this is achieved by the penetration of the alkaline ions into the fiber-matrix interface leading to a serious degradation of the unidirectional laminates of the FRP composite. However, the presence of temperature as an accelerating factor accentuated its efficiency accelerating and boosting the reaction between the alkaline ions and the matrix chemical structures.

For the case of moist concrete-encased BFRP bars, three-month conditioned samples exhibited relatively lower tensile strength reductions (compared to the other exposure periods) of 5, 6, and 12% at 20, 40, and 60^{o}C respectively. The uppermost reduction percentage recorded for the six-month specimens was 12% when it's subjected to 60^{o}C. Nine-month conditioned samples exhibited tensile strength reductions of 9, 10, and 14% at 20, 40, and 60^{o}C respectively. The residual tensile strength of BFRP bars has experienced significant drops because of the matrix softening and fiber-matrix interfacial deboning due to the hydrolysis reaction and penetration of water molecules. However, this effect was more distinct at higher temperatures and

exposure periods. Higher temperatures accelerate and enhance the hydrolysis reaction which weakens the fiber-matrix bonds causing decreases in tensile strength retention.

This research aims to compare the effect of moist concrete and alkaline environment. The concrete-encased samples were immersed in water to perfectly simulate the alkaline nature of concrete and its effect on the BFRP. The results accentuated that, in terms of tensile retention of bars, the alkaline environment was more severe than the moist concrete environment. As illustrated in Figures 4-28 and 4-29, taking the extreme temperature and greatest exposure period into account for comparison, bars conditioned for 9 months at 60^{o}C in alkaline environment experienced 29% degradation in tensile strength, while the corresponding samples in the other type of exposure experienced 14%. It can be concluded that, taking into consideration the same temperature level and exposure periods, alkaline environment was more severe than the moist concrete environment, and caused more serious degradation for the fiber-matrix interface, and interfacial debonding.

Temperature, as an accelerating factor, showed a more distinct, thorough, and accelerating effect than the duration. The higher temperature, the higher rate of ions diffusion, the higher swelling and hydrolysis rate of reaction, and that leads to higher rate of degradation of the fiber-matrix interface and lower tensile retentions. Worth mentioning, along with effect of temperature, the time of exposure still governs the extent of degradation. As a conclusion and based on the analysis of data, temperature is more influential as a durability factor than the time of exposure.

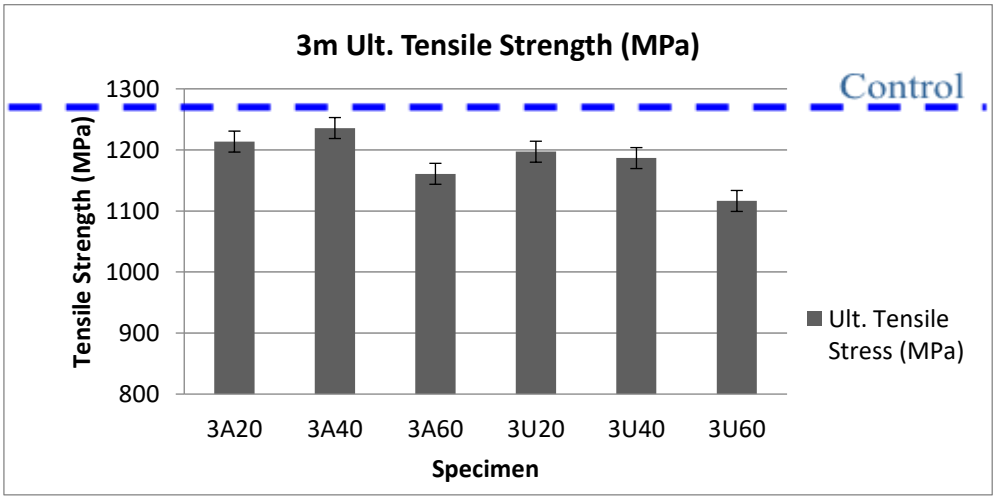

Figure 4-25: Tensile performance of 3 month-conditioned BFRP bars

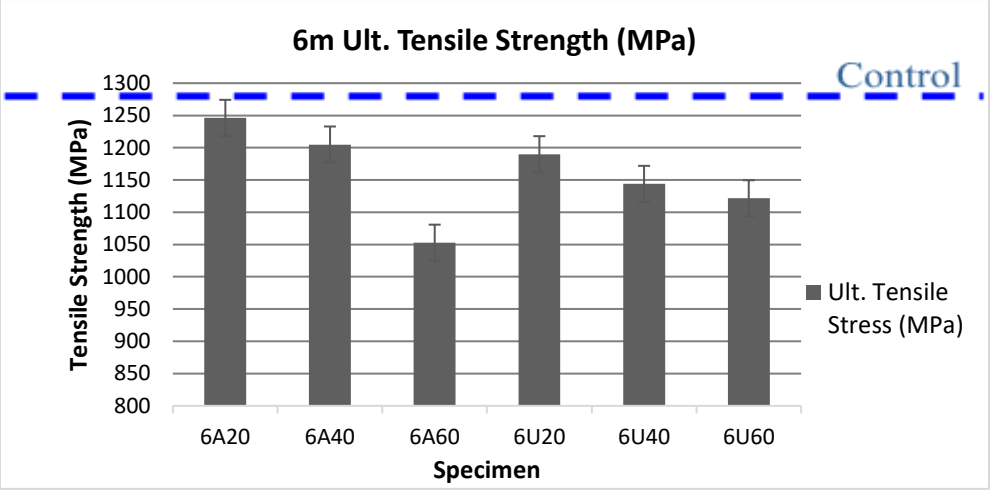

Figure 4-26: Tensile performance of 6 month-conditioned BFRP bars

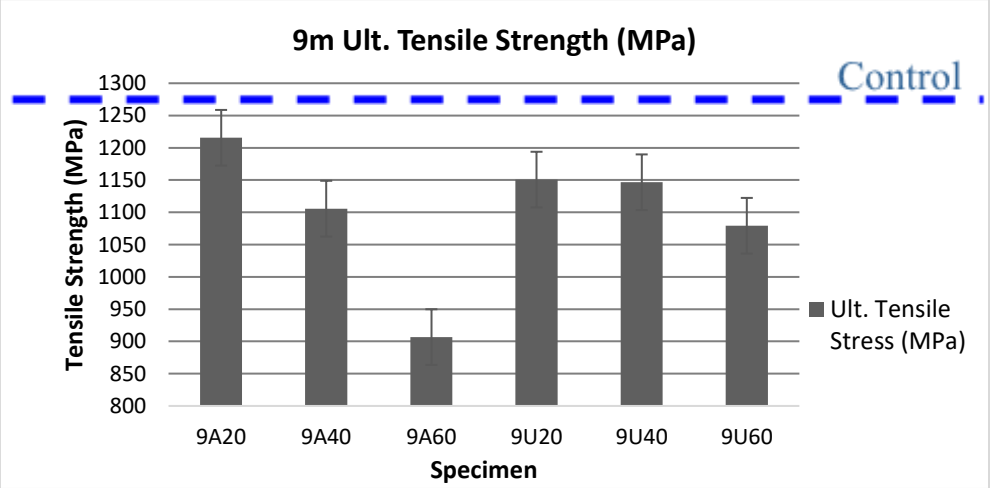

Figure 4-27: Tensile performance of 9 month-conditioned BFRP bars

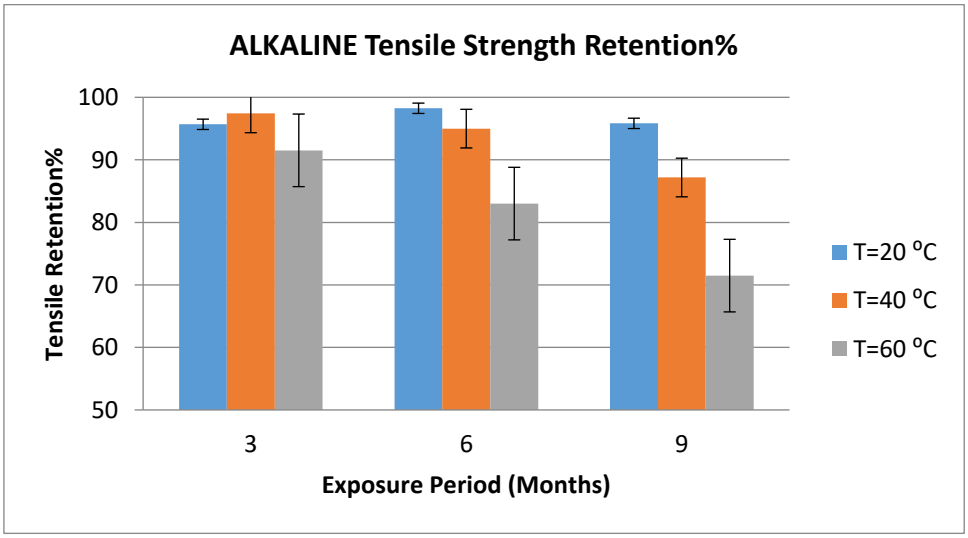

Figure 4-28: Group 1: Alkaline tensile retention based on the exposure period

El-Maaddawy et al. [24] confirmed in a previous study a similar correlation between temperature, duration, and tensile retention. The highest percentage of tensile loss recorded in El-Maaddawy et al.'s study was found to be around 50% for 9 mm-diameter GFRP bars encased by seawater-contaminated concrete and immersed in tap water for 15 months at 60°C. It was also shown that the temperature had a more distinct and efficient effect on the degradation than the exposure period. Another recent study by Benmokrane et al. [31] focused on the tensile retention of epoxy-based BFRP and vinylester-based GFRP bars conditioned for 5,000 hours in alkaline solution at 60°C. The two types exhibited different degradation performance as indicated by tensile retentions of 93% and 61% for vinylester-based GFRP, and epoxy-based BFRP respectively.

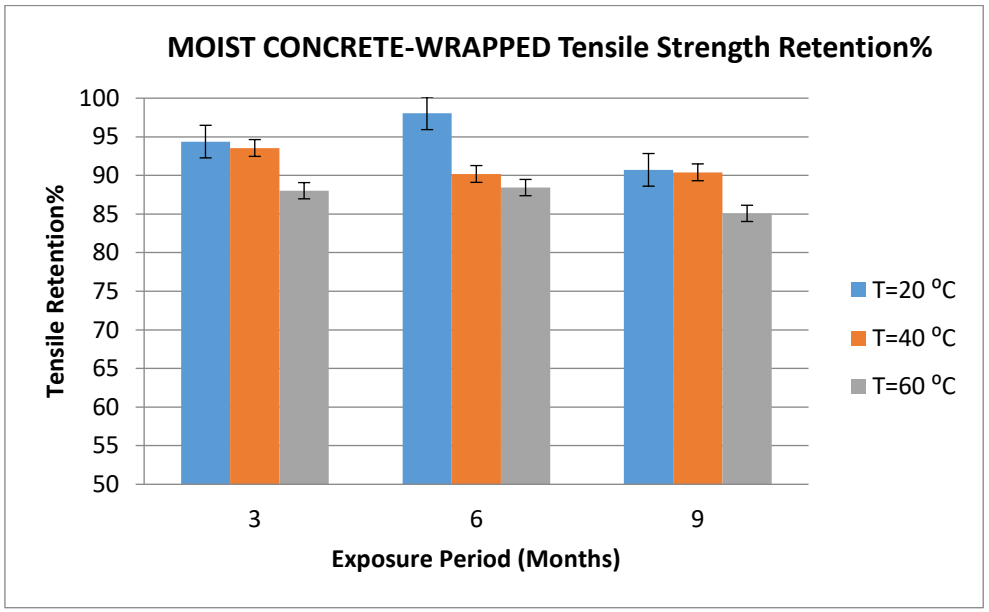

Figure 4-29: Group 2: Moist concrete tensile retention based on exposure period

4.2.2. Modulus of elasticity. The influence of harsh exposures discussed in this research on the modulus of elasticity is illustrated in Figures 4-30 and 4-31 for groups 1, and 2 respectively. The 3-month conditioned BFRP modulus of elasticity greatest drop was 13% at temperature 20°C. Moving to 6 months exposure period, BFRP modulus of elasticity exhibited a maximum increase of 19% at temperature of 60°C, as shown in Figure 4-30.

Figure 4-31 illustrates group 2 results, which stands for moist concrete-encased exposure. The 3-month conditioned BFRP modulus of elasticity greatest increase was

recorded to be 19% at temperatures 40°C. Moving to 6 months exposure period, BFRP modulus of elasticity exhibited a maximum drop of 6% at temperature of 20°C. At 3-month conditioning, the modulus of elasticity of BFRP bar was almost the same at 20 and 60°C, but decreased by 22% at 40°C. The penetration of alkaline ions into the BFRP bars causes swelling and plasticization/softening of the matrix. Swelling of matrix enhances the fiber-matrix mechanical adhesion which explains the increase in modulus of elasticity at 40°C, while the subsequent drop in tensile modulus at 60°C can be referred to the plasticization/softening effect. Swelling and softening are successive processes, but they have reverse effect on the matrix of the FRP composite. Mourad et al. [55] implied in their research paper that the reason of tensile modulus reduction can be related to the breakdown of molecular weight of the matrix due to the water-matrix reaction. Another conceivable reason for the reduction, the water could reduce the polymer chains mobility during prolonged durations which stiffens the matrix.

El-Maaddawy et al. [24] confirmed in a previous study a similar correlation between matrix and tensile modulus of elasticity. However, the modulus of elasticity exhibited increases then insignificant drops at later stages. The highest percentage of tensile modulus loss recorded in El-Maaddawy et al.'s study was found to be around 7% for 8 mm-diameter GFRP bars wrapped by seawater-contaminated concrete and immersed in tap water for 15 months at 40°C. Worth mentioning, based El-Maaddawy et al.'s results, the modulus of elasticity of GFRP bars in the first 300 day was almost unchanged. Another recent study by Benmokrane et al. [31] focused on the modulus of elasticity retention of epoxy-based BFRP and vinylester-based GFRP bars conditioned for 5,000 hours in alkaline solution at 60°C. Both types showed almost a similar degradation performance as indicated by retentions of 81% and 86% for vinylester-based GFRP, and epoxy-based BFRP respectively.

4.2.3. Failure mode. All the specimens' failure modes were represented by globalized detaching and debonding of the fibers as shown in Figure 4-32. Few BFRP specimens experienced a premature failure at the end grips due to the high rate of loading, or the insufficient bond strength between the BFRP bar surface and nano-grout used as filler in the grips. All specimens which exhibited premature failure were disregarded as their results were not reliable. Table 4-8 lists the specimens which exhibited a premature failure.

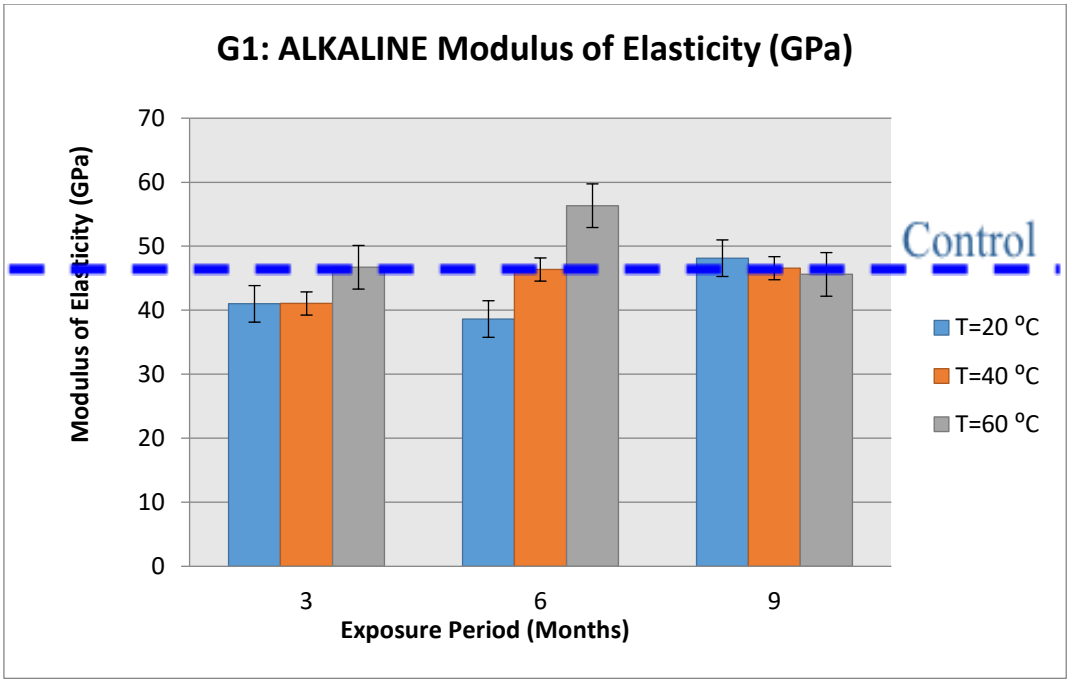

Figure 4-30: Group 1: Alkaline moduli of elasticity

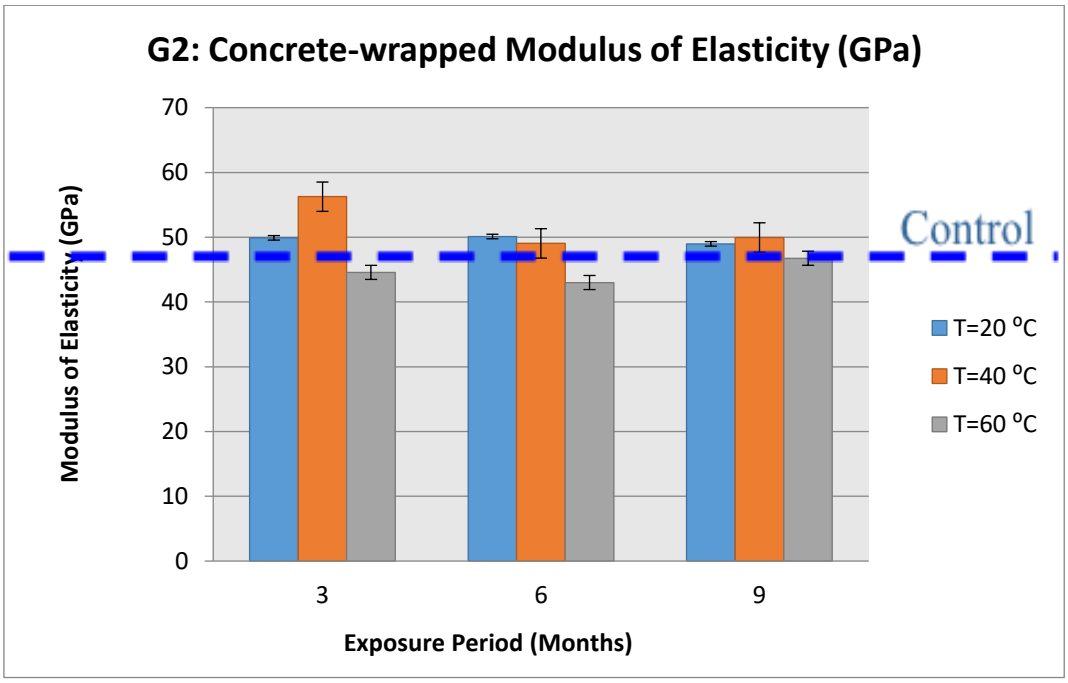

Figure 4-31: Group 2: Moist concrete moduli of elasticity

Table 4-8: Premature-failed BFRP specimens

Specimen	Type of Exposure	Exposure Duration (Months)	Temperature (°C)	Replicate no.
3A20_3	Alkaline	3	20	3
6A60_1	Alkaline	6	60	1
6U60_3	Moist concrete-wrapped	6	60	3

Figure 4-32: Detaching of fibers due to tensile failure

4.3. SEM Analysis

This section discusses effect of the different types of exposures on the microstructural level compared to the level of degradation, based on the temperature and time of exposure. The test program of SEM was selected to showcase the comparisons of the different conditioning effects, temperatures as an accelerating factor, and time of exposure. SEM enables the researcher to examine the longitudinal and cross-sectional micro-cracks and separations in the matrix, or fiber-matrix interface. However, it also enables to evaluate chemical resistance, and physical endurance of the BFRP bars.

Figures 4-33 to 4-34 illustrate the temperature effect of conditioned samples for nine months in alkaline solution. Figures 4-33a, 4-33b, 4-34a, and 4-34b for control and 9A20 samples, show a fair bonding and adhesion between the fibers and matrix, also indicating no micro-cracks, separations, fiber smoothening, matrix deterioration/disintegration. This explains the minimal loss of tensile strength as discussed previously. Looking into Figures 4-33c, 4-33d, 4-34c, and 4-34d for 9A40 and 9A60, this phase was associated with major circumferential and longitudinal micro-cracks and separations. The micro-gaps ranged from 1 to 2 μm in the cross-sectional view, while it ranged from 2 to 5 μm as a longitudinal separation due to the fiber-matrix debonding. This phenomenon resulted because of the major hydrolysis process, alkaline ions ingress, and the unequal distribution of load among the fibers. The non-uniform load is caused by high temperatures. The fibers conditioned for 9 months at 60^{o}C experienced noticeable crack propagation and a substantial degradation of matrix. This supports the major losses in tensile retention as proven in section 4.2.1 [35].

The temperature effect of conditioned concrete-encased samples for nine months in normal water is illustrated in Figures 4-35 to 4-36. The figures show an approximately similar performance of the previously mentioned group (alkaline), with minor micro-cracks, debonding, and softening for those conditioned at 20^{o}C, and a major development of micro-cracks, gaps, debonding, and degradation in the fiber-matrix interface for those conditioned at 60^{o}C. The 60^{o}C environment showed a relatively more aggressive effect than the 40^{o}C environment.

Figures 4-37 to 4-38 elucidate the effect of exposure period BFRP samples conditioned at 40^{o}C in alkaline solution. The effect of 9-month time of exposure, as shown in Figures 4-37d and 4-38d, is represented by localized etching and debonding due to the long-term penetration of alkaline ions, weakening and disintegrating the chemical bonds at the fiber-matrix interface, leading to a serious degradation of the unidirectional laminates of the FRP composite. Those BFRP samples exhibited major micro-cracking. and separations. width of the circumferential micro-crack was found

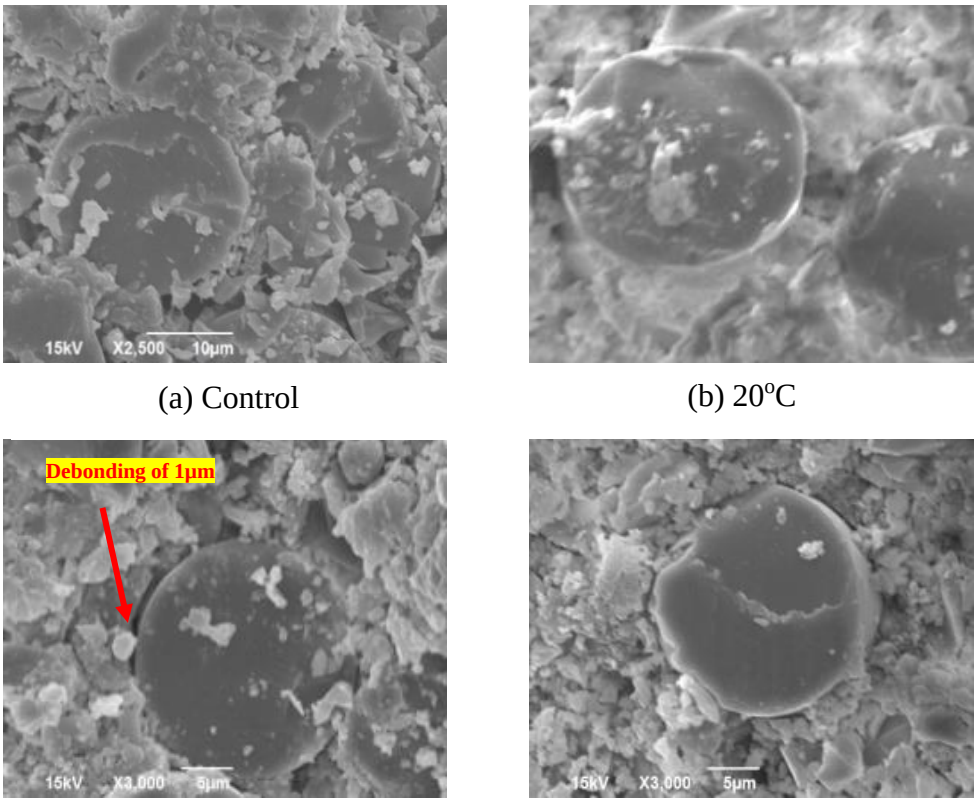

(a) Control (b) 20^{o}C

(c) 40^{o}C (d) 60^{o}C

Figure 4-33: Cross-sectional micrograph of BFRP specimens immersed in alkaline for 9 months at different temperatures

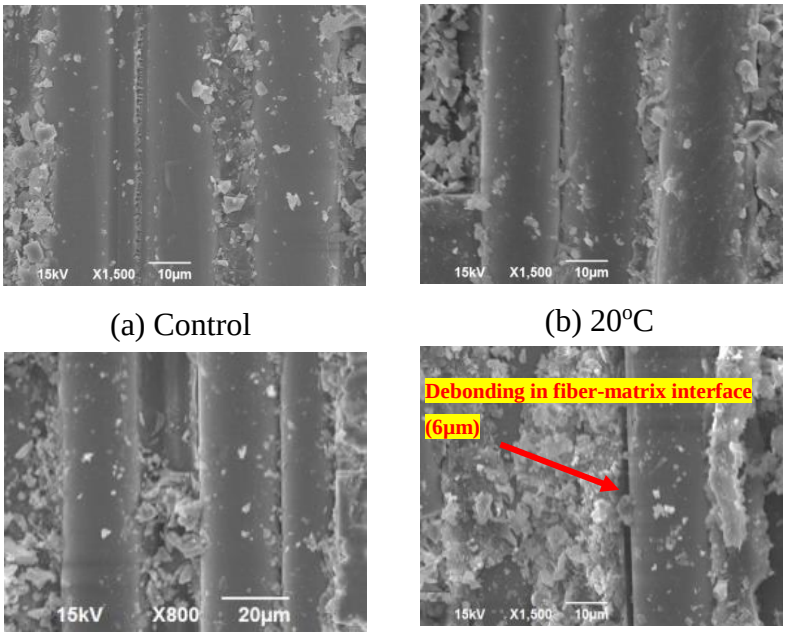

(a) Control (b) 20°C

(c) 40°C (d) 60°C

Figure 4-34: Longitudinal micrograph of BFRP specimens immersed in alkaline for 9 months at different temperatures

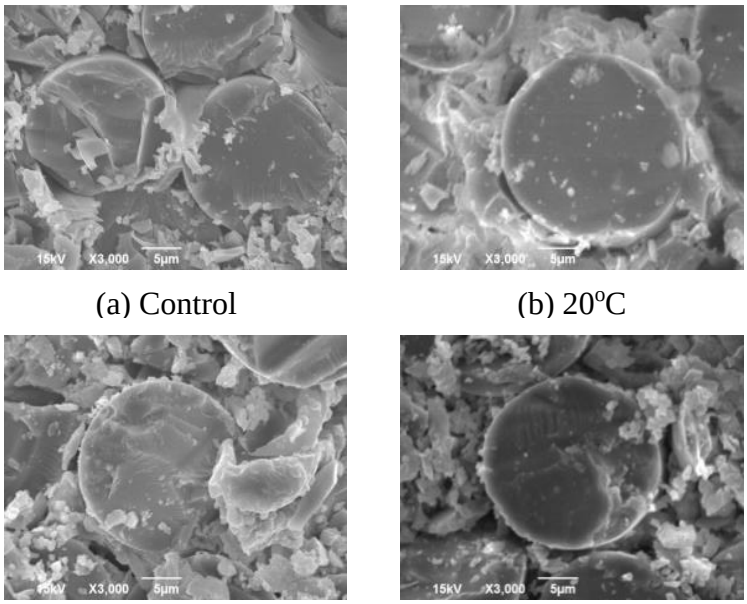

(a) Control (b) 20°C

(c) 40°C (d) 60°C

Figure 4-35: Cross-sectional micrograph of moist concrete-encased BFRP specimens for 9 months at different temperatures

to be around 0.5 µm, while the width of a longitudinal gap was found to be 1.5 µm. This indicated that the degradation of the fiber-matrix interface was not severely intensified with prolonged intervals of exposure. It was concluded that the BFRP bars

were more susceptible to the degradation effect of temperature than the time of exposure as proven previously in section 4.2.1.

Similar performance was noticed for the case concrete-encased conditioning as shown in Figures 4-39 to 4-40, which demonstrate the time of exposure effect for samples conditioned at 40°C in normal water.

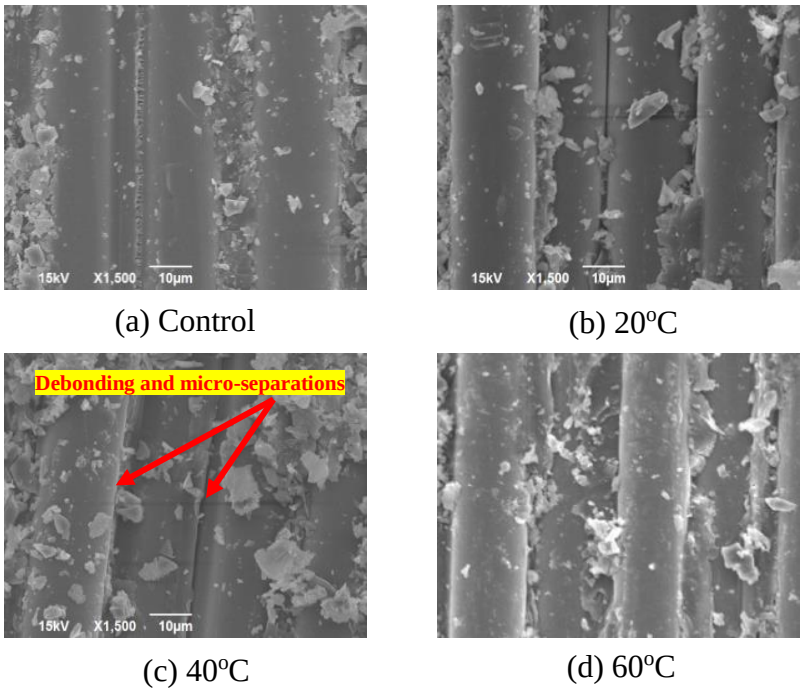

(a) Control (b) 20°C

(c) 40°C (d) 60°C

Figure 4-36: Longitudinal micrograph of moist concrete-encased BFRP specimens for 9 months at different temperatures

The results indicate minor micro-cracks, debonding, and softening for those conditioned for 3 months. However, a major development of micro-cracks, gaps, debonding, and degradation in the fiber-matrix interface was shown for those conditioned for 9 months. The nine-month duration of exposure showed a relatively more aggressive effect than the three-month duration [8, 53].

Benmokrane et al. [31] confirmed in a previous study a similar relationship between temperature, duration, and debonding of fibers. It was proven that, the more severe the conditioning was, the greater the debonding and micro-separation in the fiber-matrix interface resulted in. Another study by El-Hassan et al. [35] showed that the GFRP bars was more susceptible to the temperature as a durability factor than exposure period. Micro-separations and matrix disintegration were detected in both types of GFRP. Moreover, SEM images detected substantial micro-separation

propagation in 60°C-conditioned samples, and the width of separation was recorded to be around 6 µm.

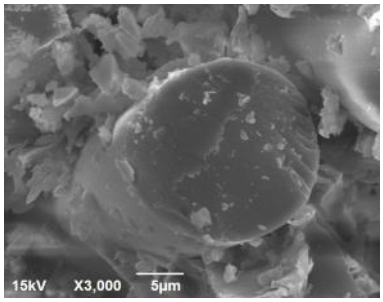

(a) 3 months

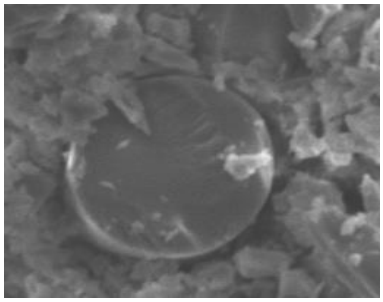

(b) 6 months

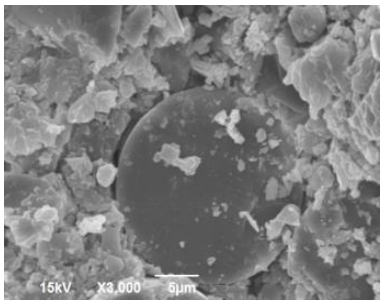

(c) 9 months

Figure 4-37: Cross-sectional micrograph of BFRP specimens immersed in alkaline for certain exposure durations at 40°C

4.4. Matrix Digestion Analysis

Matrix digestion analysis helps determine the percentages of fibers and matrix (epoxy) of a BFRP. The test was conducted on control and conditioned specimens, so the matrix loss is monitored; hence, the effect of the conditioning and level of deterioration can be evaluated. Matrix digestion by nitric acid method was used in which it is based on the dissolution of the conditioned specimen mass. Table 4-9 lists the percentages of matrix and fiber of various conditioned and unconditioned samples. Generally, greater exposure durations and temperatures tended to cause higher matrix loss. In fact, the SEM images showed matrix cracking and abrasion after 9 months of conditioning which validates the results obtained in matrix digestion by nitric acid. This cracking and abrasion are represented by a matrix loss at the fiber-matrix interface in the results. As observed in Table 4-9, the alkaline-exposed specimens (G1) were more susceptible to degradation, localized micro-cracking, and most importantly, matrix loss.

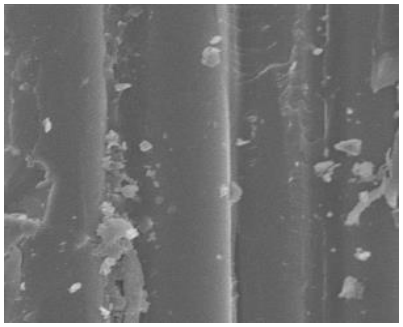

(a) 3 months

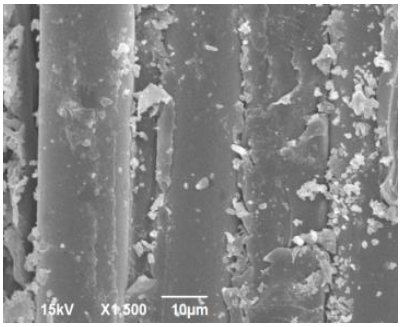

(b) 6 months

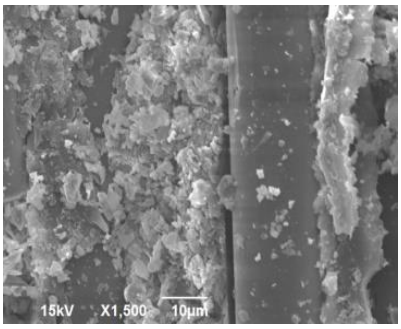

(c) 9 months

Figure 4-38: Longitudinal micrograph of BFRP specimens immersed in alkaline for different exposure durations at 40^{o}C

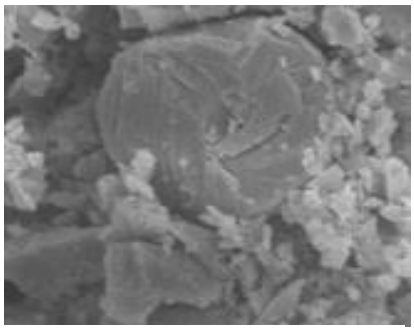

(a) 3 months

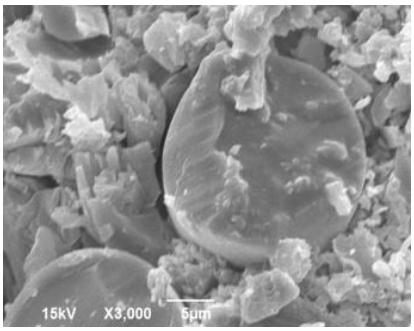

(b) 6 months

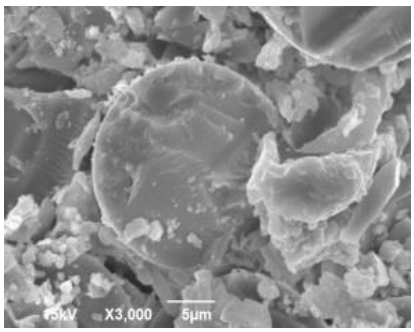

(c) 9 months

Figure 4-39: Cross-sectional micrograph of moist concrete-encased BFRP specimens immersed for different exposure durations at 40^{o}C

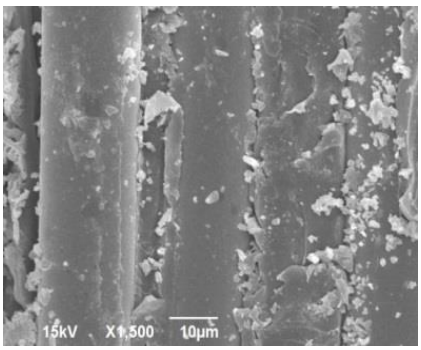

(a) 3 months

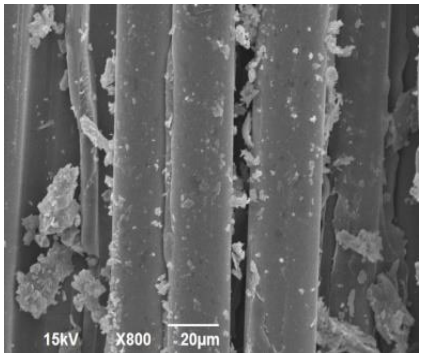

(b) 6 months

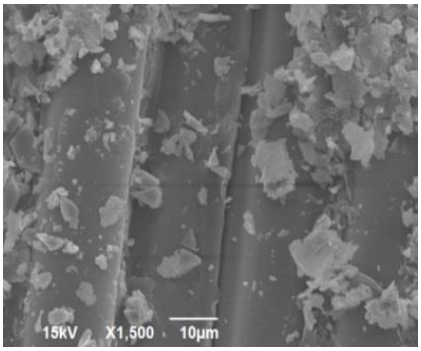

(c) 9 months

Figure 4-40: Longitudinal micrograph of moist concrete-encased BFRP specimens immersed for different exposure durations at 40°C

Table 4-9: Matrix loss determined by matrix digestion method

Exposure Type: Group no.	Conditioning		Content%		Matrix Loss%
	Duration (month)	Temperature °C	Fiber	Matrix	
Alkaline: G1	Control	Ambient	74.5	25.5	-
	9	60	82.1	17.9	29.8
Moist concrete-encased: G2	Control	Ambient	74.5	25.5	-
	9	60	81.2	18.8	26.2

El-Hassan et al. [35] indicated that, with the increase of temperature and exposure period, the matrix loss increases, which confirmed the current observations discussed above. The highest percentage of matrix loss recorded in El-Hassan et al.'s research was found to be around 38% for 9 mm-diameter GFRP bars wrapped by seawater-contaminated concrete and immersed in tap water for 15 months at 60°C. Benmokrane et al. [31] exposed epoxy-based BFRP bars in alkaline solution for 7 days at 96°C, however, the mass loss recorded was found to be 0.9%.

4.5. FTIR Analysis

As discussed earlier, FTIR analysis is used to evaluate the level of hydrolysis reaction occurred while conditioning. Knowing that, the hydrolysis increases the band of OH infrared band, while it does not influence the CH band. The studied regions were; carbon-hydrogen groups (CH): 2800‑3000 cm^{-1} and hydroxyl groups (OH): 3200‑3600 cm^{-1}. The ratio of maximum peaks in each of CH and OH band illustrates the relative amount of hydroxyl groups in the specimen [20, 32]. CH is represented by the peaks at 2800-3000 cm^{-1}, while OH can be found at 3200-3600 cm^{-1} peaks in the intensity plots (Figures 4-41 and 4-42). The intensity of CH peaks typically does not change because of conditioning. It may slightly vary from sample to sample as a variation in the FRP production. FTIR spectra of control and conditioned samples for different exposure periods and exposed temperatures are plotted in Figures 4-41 and 4-42. The OH/CH ratio is the maximum intensity peak in OH divided by the maximum intensity peak in CH. Table 4-10 shows the OH/CH ratio of the specimens tested along with the increase percentage which represents the change in OH/CH ratio of conditioned samples with respect to that of control sample. It was observed from Table 4-10 that the higher the temperature, the more significant the hydrolysis reaction takes place. Regarding the type of exposure, it was concluded from the results that, the hydrolysis reaction progressed more severely in alkaline environments than the natural concrete environment, and that complies with tensile strength results. The higher the temperature, the greater the formation of conditioning-induced hydroxyl groups. However, the temperature effect was deficient in this case due to the relatively short duration of exposure. On the other hand, the exposure duration factor effect was more distinct, with the increase of exposure period, the hydrolysis progressed more evidently. The insignificant reduction in tensile strength of most of the specimens may explain the insignificant difference in OH/CH ratios.

The above finding coincides with El-Hassan et al. [35] results, where the increase of temperature intensifies the hydrolysis reaction. The highest percentage of OH/CH increase recorded in El-Hassan et al.'s research was found to be around 97% for GFRP bars wrapped by seawater-contaminated concrete and immersed in tap water for 15 months at 40^{o}C. Also, the OH groups were induced due to the hydrolysis reaction,

hence, breakdown of matrix polymers caused impairments in the fiber-matrix interface bond.

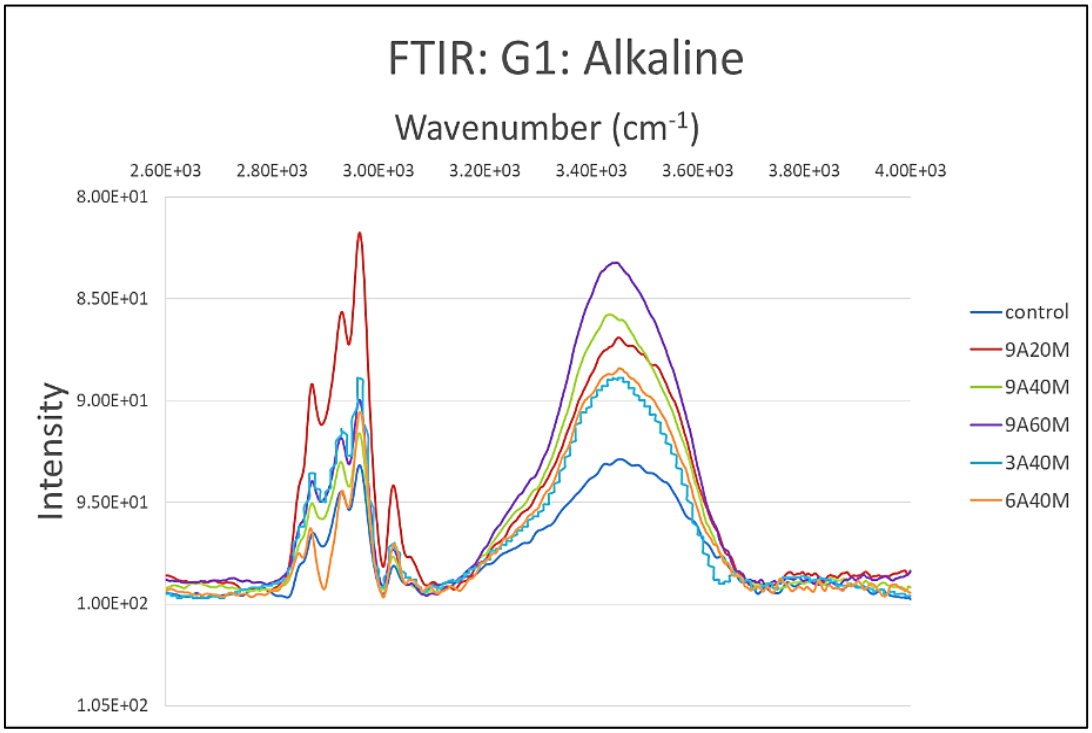

Figure 4-41: FTIR wave intensity for alkaline specimens

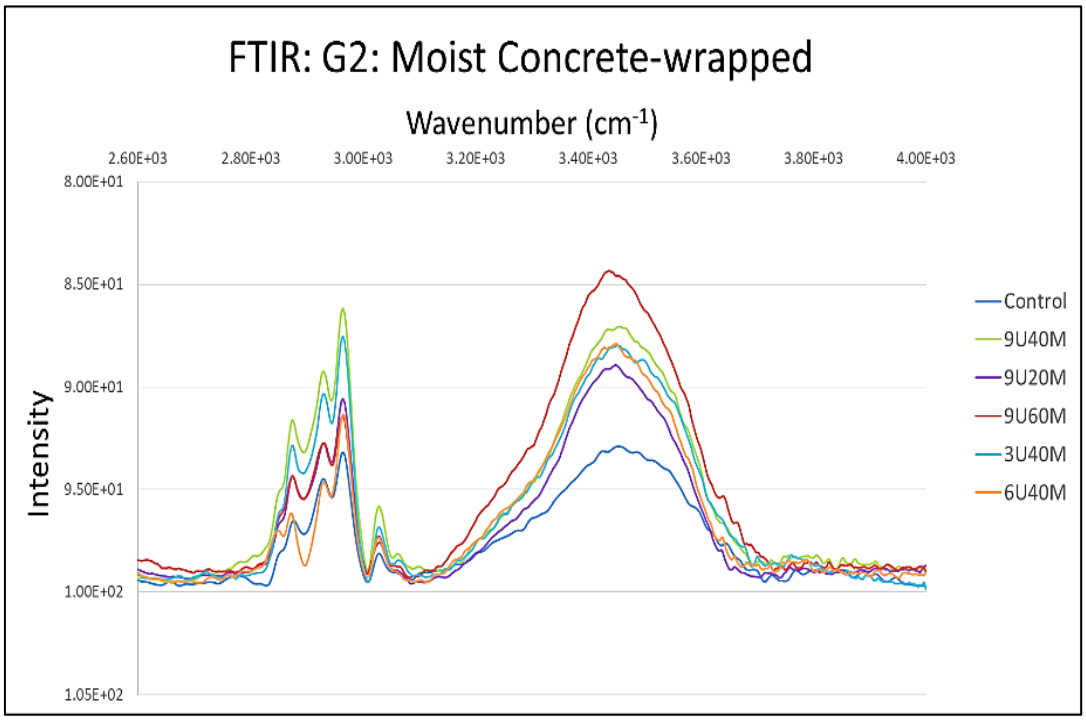

Figure 4-42: FTIR wave intensity for concrete-wrapped specimens

Table 4-10: OH/CH obtained from FTIR test

Surrounding media	Tag Name	Temperature(°C)	Time of Exposure (Months)	CH Intensity	OH Intensity	OH/CH	Increase%
Control	C	-	-	9.3	9.35	1.01	-
Alkaline	3A40M	40	3	8.82	8.9	1.01	0
	6A40M	40	6	9.075	8.85	0.98	3
	9A20M	20	9	8.23	8.7	1.06	5
	9A40M	40	9	9.2	8.75	0.95	5
	9A60M	60	9	9.5	8.15	0.86	15
Unloaded Moist Encased-concrete bars	3U40M	40	3	8.7	8.78	1.01	0
	6U40M	40	6	9.17	8.85	0.97	4
	9U20M	20	9	9.6	8.95	0.93	7
	9U40M	40	9	8.3	8.9	1.07	7
	9U60M	60	9	9.15	8.2	0.90	11

4.6. DSC Analysis

The DSC analysis determines the glass transition temperature (T_g) of the conditioned BFRP samples. ASTM E1356 was followed to obtain the resultant glass temperature (T_g). Two runs were conducted on the specimens; the first scan or run is mostly used to remove any residuals or impurities and the thermal history of the sample. Values of T_g are presented in Table 4-11. As the results show, the samples conditioned in higher temperatures exhibited a lower T_g after the first scan, this could be related to the plasticization of matrix, and the micro voids and separations in the fiber-matrix interface, however, the SEM imaging confirms that. The polymer in BFRP was introduced to moisture, whereby the polymer matrix absorbed the moisture and caused an alteration in its properties, so the T_g decreases as a result [50].

Taking the exposure period into consideration, specimens conditioned at the same temperature but for different exposure periods exhibited change in the T_g, however, a lower T_g with the greater period of exposure. The trend of T_g with respect to exposure period showed somewhat an equilibrium state in later stages. Taking the temperature into consideration, higher temperatures intensified the diffusion rate of absorption, more micro-cracks developed, and hence, more plasticization took place. Both types of exposure resulted in almost similar effect on T_g .

In the 2nd run, specimens exhibited post-curing during heating, in other words, heating caused water evaporation, which reversed the plasticization. That explains why the T_g values are equal to those of control specimens.

El-Hassan et al. [35] study showed similar response where the increase of temperature and exposure period increased the glass transition temperature (T_g). The lowest T_g recorded in the 1st run by El-Hassan et al was found to be 90°C for GFRP bars encased by seawater-contaminated concrete and immersed in tap water for 15 months at 60°C. Also, matrix polymers exhibited an alteration in the chemical and thermal properties which was reflected by the change in T_g. The 2nd run T_g, confirming with this research conclusion, was similar to those of control specimens (around 106°C and 126°C for type I and II respectively) due to post-curing and reversed plasticization effect. Another recent study by Benmokrane et al. [31] studied the T_g, as a degradation indicator of epoxy-based BFRP and vinylester-based GFRP bars conditioned for 5,000 hours in alkaline solution at 60°C. The two types exhibited different T_g of 111°C and 112°C for vinylester-based GFRP, and epoxy-based BFRP respectively, where the T_g of control ones were recorded to be 102°C and 116°C respectively. As noticed, T_g values for the vinylester-based GFRP bars increased due to post-curing, whereas T_g for epoxy-based BFRP exhibited a slight increase due to matrix softening.

Table 4-11: Glass temperature of control and conditioned specimens obtained by DSC analysis

Surrounding media	Temperature(°C)	Time of Exposure (Months)	Tag Name	1st Run Tg (°C)	1st Run Tg (°C)
Control			C	125	124
Alkaline	40	3	3A40M	112	124
		6	6A40M	77	118
	20	9	9A20M	65	105
	40		9A40M	85	125
	60		9A60M	75	124
Unloaded Moist Encased-concrete bars	40	3	3U40M	115	124
		6	6U40M	75	121
	20	9	9U20M	85	128
	40		9U40M	54	120
	60		9U60M	65	125

Chapter 5. Summary, Conclusion, and Recommendations

The durability performance of BRFP bars has been investigated in this research, where a set of bare bars were conditioned in alkaline solution, and another set of concrete-encased bars were exposed to normal water. Certain tests were implemented before and after conditioning to evaluate the mechanical and microstructural properties for BFRP bars. The output of these tests provides a comprehensive microstructural characterization and tensile behavior evaluation before and after exposure to the harsh environments mentioned above. Thorough micro-structural and chemical testing were conducted to support the results obtained from the mechanical tests. Plasticization, hydrolysis, fiber debonding, micro-separations, micro-cracks, and loss of matrix were observed in SEM images and chemical analyses as potential causes for durability deterioration. Although this research concluded remarks that are limited to the specimens tested, the methodology and results can be adopted to develop durability models for the BFRP to predict the tensile strength and other parameters. The main findings, concluding remarks, and recommendations for future work are highlighted in this chapter.

Results in this research study provide an insight and comparison between two different exposures; temperature and exposure period. However, these two factors were investigated in depth in terms of efficiency and severity on the durability. Degradation for the moist concrete-encased specimens is highly dependent on the concrete properties such as, void content, threshold, absorption, production quality, and the fiber composite characteristics. The bare bars (subjected to alkaline conditioning) degradation is dependent on the BFRP chemical composition, manufacturing process, interfacial characteristics. The compatibility between tensile strength results and microstructural tests, as stated in the discussion chapter, confirms the validity of tensile results. The following findings are drawn:

1. Unlike the concrete-wrapped BFRP specimens, BFRP bars immersed in the alkaline environment exhibited greater moisture uptake percentages as they are exposed directly to the aqueous solution. Maximum moisture uptake percentage was found to be 1% for both alkaline and Concrete-wrapped groups. As the duration of conditioning increases, the aqueous molecules continue to penetrate

and diffuse through the cracks and gaps been propagated resulting in a greater moisture uptake. The temperature as an accelerating factor increased the rate of diffusion into the FRP matrix capillaries. The moisture uptake kept increasing until the BFRP reaches an equilibrium state of saturation.

2. For the same temperature level and exposure period, alkaline environment was more severe than moist concrete environment, and caused more serious degradation for the fiber-matrix interface, and interfacial depending. Temperature was found to be more influential as a durability factor than the time of exposure. It showed a more distinct, thorough, and accelerating effect than the duration.
3. The penetration of alkaline ions into the BFRP bars causes swelling and plasticization/softening of the matrix. Swelling of matrix enhances the fiber-matrix mechanical adhesion which explains the increase in modulus of elasticity in higher temperatures.
4. Tensile strength testing revealed that the BFRP samples subjected to 20^{o}C in alkaline environment exhibited a lower reduction in tensile strength than the other environmental temperatures. On the other hand, The uppermost reduction percentages recorded for the 3-, 6- and 9-month specimens were 12, 14, and 29%, respectively, when exposed to the highest temperature of 60^{o}C. . The residual tensile strength of BFRP bars has experienced significant drops in the most extreme cases because of the matrix softening and fiber-matrix interfacial deboning due to the hydrolysis reaction.
5. It can be concluded from the SEM micro-imaging that the fibers conditioned for 9 months at 60^{o}C experienced noticeable crack propagation and a substantial degradation of matrix. This supports the major losses in tensile retention. The results indicated minor micro-cracks, debonding, and softening for those conditioned at 20^{o}C. On the other hand, a major development of micro-cracks, gaps, debonding, and degradation in the fiber-matrix interface was shown in those conditioned at 60^{o}C. The 60^{o}C environment showed a relatively more aggressive effect than the 40^{o}C environment. The BFRP bars were more susceptible to the degradation effect of temperature than the time of exposure. The nine-month duration of exposure showed a relatively more aggressive effect than the three-month duration.

6. Matrix digestion analysis proved that greater exposure durations and temperatures tended to cause higher matrix loss. In fact, SEM images showed matrix cracking and abrasion after 9 months of conditioning which validated the results obtained in matrix digestion by nitric acid.
7. FTIR analysis indicated that the higher the temperature, the more significant the hydrolysis reaction takes place. The hydrolysis reaction progressed more severely in alkaline environments than the natural concrete environment, and that complies with tensile strength results. Temperature effect was insignificant in this case due to the relatively short duration of exposure. On the other hand, the exposure duration factor effect was more distinct, with the increase of exposure period, the hydrolysis progressed more evidently.
8. From the DSC analysis results, it was indicated that the samples conditioned in higher temperatures exhibited a lower T_g after the first scan. This could be related to the plasticization of matrix and the micro voids and separations in the fiber-matrix interface, as confirmed by the SEM images.

Recommendations for future study can be summarized as follows:

- To develop a durability model which enables the researcher to predict parameters of FRP composite. This requires collections of many set of data to provide accurate prediction of the long-term durability response for this type of composites.
- To investigate the durability of moist concrete-encased BFRP bars subjected to sustained loading in harsh environments. Different levels of sustained load could be considered.
- To include the acidic environment as a harsh exposure, so a comparative study can be conducted on these cases.

References

[1] ACI 440.3R-04. *Guide test methods for fiber-reinforced polymers (FRPs) for reinforcing or strengthening concrete structures*. American Concrete Institute 440 Committee. 2004.

[2] L. Hollaway, "A review of the present and future utilisation of FRP composites in the civil infrastructure with reference to their important in-service properties," *Construction and Building Materi*als, vol. 24, no. 12, pp. 2419–2445, 2010.

[3] N. Uddin, A. Abro, J. Purdue, and U. Vaidya, "Thermoplastic composites for bridge structures," *Developments in Fiber-Reinforced Polymer (FRP) Composites for Civil Engineering*, vol. 3, no.5, pp. 50–65, 2013.

[4] C. E. Bakis, L. C. Bank, V. L. Brown, E. Cosenza, J. F. Davalos, J. J. Lesko, A. Machida, S. H. Rizkalla, and T. C. Triantafillou, "Fiber-Reinforced Polymer Composites for Construction—State-of-the-Art Review," *Journal of Composites for Construction*, vol. 6, no. 2, pp. 73–87, 2002.

[5] ASTM D7565 / D7565M-10, *Standard Test Method for Determining Tensile Properties of Fiber Reinforced Polymer Matrix Composites Used for Strengthening of Civil Structures*. ASTM International, West Conshohocken, PA, 2017.

[6] H. Brothers. *Glass Fiber Reinforced Polymer (GFRP) Dowel Bars*. Hughes Brothers, 2011.

[7] F. Ceroni, E. Cosenza, M. Gaetano, and M. Pecce, "Durability issues of FRP rebars in reinforced concrete members," *Cement and Concrete Composites*, vol. 28, no. 10, pp. 857–868, 2006.

[8] M. Montaigu, M. Robert, E. A. Ahmed, and B. Benmokrane, "Laboratory Characterization and Evaluation of Durability Performance of New Polyester and Vinylester E-glass GFRP Dowels for Jointed Concrete Pavement," *Journal of Composites for Construction*, vol. 17, no. 2, pp. 176–187, 2013.

[9] M. Schürch, "GFRP Soft-Eye for TBM Breakthrough: Possibilities with a Modern Construction Material," in *International Symposium on Underground Excavation and Tunnelling*, 2006, pp. 4–9.

[10] S. Matthys, M. Tierens, and A. Palmieri, "Basalt fibres," *Concrete Solutions*, vol. 14, no. 2, pp. 29–51, 2009.

[11] K. Van de Velde, P. Kiekens, and L. Van Langenhove, "Basalt fibres as reinforcement for composites," in *Proceedings of 10th international conference on composites/nano engineering*, 2003, pp. 1–6.

[12] C. Soutis, "Carbon fiber reinforced plastics in aircraft construction," *Materials Science and Engineering: A*, vol. 412, no. 2, pp. 171–176, 2005.

[13] Z. Wu, X. Wang, and G. Wu "Advancement of basalt fiber composites towards infrastructural applications," in *Proceedings of ISISS2011*, 2011, pp. 28–33.

[14] G. Wu, Z.-Q. Dong, X. Wang, Y. Zhu, and Z.-S. Wu, "Prediction of Long-Term Performance and Durability of BFRP Bars under the Combined Effect of Sustained Load and Corrosive Solutions," *Journal of Composites for Construction*, vol. 19, no. 3, pp. 12–16, 2015.

[15] J. Sim, C. Park, and D. Y. Moon, "Characteristics of basalt fiber as a strengthening material for concrete structures," *Composites Part B: Engineering*, vol. 36, no. 6-10, pp. 504–512, 2005.

[16] M. Dawood and S. Rizkalla, "Environmental durability of a CFRP system for strengthening steel structures," *Construction and Building Materials*, vol. 24, no. 9, pp. 1682–1689, 2010.

[17] T. Nguyen, Y. Bai, X. Zhao, and R. Al-Mahaidi, "Durability of steel/CFRP double strap joints exposed to sea water, cyclic temperature and humidity," *Composite Structures*, vol. 94, no. 5, pp. 1834–1845, 2012.

[18] B. Wan, M. F. Petrou, and K. A. Harries, "The Effect of the Presence of Water on the Durability of Bond between CFRP and Concrete," *Journal of Reinforced Plastics and Composites*, vol. 25, no. 8, pp. 875–890, 2006.

[19] Y. Chen, J. F. Davalos, and I. Ray, "Durability Prediction for GFRP Reinforcing Bars Using Short-Term Data of Accelerated Aging Tests," *Journal of Composites for Construction*, vol. 10, no. 4, pp. 279–286, 2006.

[20] M. Robert, P. Cousin, and B. Benmokrane, "Durability of GFRP reinforcing bars embedded in moist concrete," *Journal of Composites for Construction*, vol. 13, no.2, pp. 66-73, 2009.

[21] H. Kim, Y. Park, Y. You, and C. Moon. "Short-term durability test for GFRP rods under various environmental conditions," *Composite structures*, vol. 83, no.1, pp. 37-47, 2008.

[22] W. Mingchao, Z. Zuoguang, L. Yubin, L. Min, and S. Zhijie, "Chemical Durability and Mechanical Properties of Alkali-proof Basalt Fiber and its Reinforced Epoxy Composites," *Journal of Reinforced Plastics and Composites*, vol. 27, no. 4, pp. 393–407, 2008.

[23] G. Wu, X. Wang, Z. Wu, Z. Dong, and G. Zhang, "Durability of basalt fibers and composites in corrosive environments," *Journal of Composite Materials*, vol. 49, no. 7, pp. 873–887, 2014.

[24] T. El-Maaddawy, and A. Al-Saidy, "Residual Strength of Glass FiberReinforced Polymer Bars in Seawater-Contaminated Concrete," in *Proceedings of the Fifth International Conference on Construction Materials (ConMat' 15): Performance, Innovations and Structural Implications*, 2015, pp. 19-23.

[25] A. El Refai and F. Abed, "Concrete Contribution to Shear Strength of Beams Reinforced with Basalt Fiber-Reinforced Bars", *Journal of Composites for Construction*, vol. 20, no. 4, pp. 393–407, 2016.

[26] F. Abed, H. El-Chabib, and M. AlHamaydeh, "Shear characteristics of GFRP-reinforced concrete deep beams without web reinforcement," *Journal of Reinforced Plastics and Composites*, vol. 31, no. 16, pp. 1063-1073, 2012.

[27] A. Tamimi, F. Abed, and A. Al-Rahmani, "Effects of harsh environmental exposures on the bond capacity between concrete and GFRP reinforcing bars," *Advances in Concrete Construction, An International Journal*. vol. 2, no. 1. pp. 1-11, 2014.

[28] A. E. Refai, F. Abed, and A. Altalmas, "Bond Durability of Basalt Fiber–Reinforced Polymer Bars Embedded in Concrete under Direct Pullout Conditions," *Journal of Composites for Construction*, vol. 19, no. 5, pp. 523–625, 2015.

[29] S. Alhamad, Y. A. Banna, A. Osman, S. Mouthassseeb, J. Abdalla, and F. Abed, "*Effect of shear span-to-depth ratio on the shear behavior of BFRP-RC deep beams*," vol. 5, no. 1, pp. 545–600, 2017.

[30] F. Abed, A. R. Alhafiz, "Effect of basalt fibers on the flexural behavior of concrete beams reinforced with BFRP bars," *Composite Structures*, vol. 215, no. 2, pp. 23-34, 2019.

[31] B. Benmokrane, F. Elgabbas, E. Ahmed and P. Cousin, "Characterization and Comparative Durability Study of Glass/Vinylester, Basalt/Vinylester, and Basalt/Epoxy FRP Bars," *Journal of Composites for Construction*, vol. 19, no. 6, pp. 115–150, 2015.

[32] H. Li, G. Xian, M. MA, and J. Wu, "Durability and Fatigue Performance of Basalt Fiber / Epoxy Reinforcing Bars," in *5th International Conference on FRP Composites in Civil Engineering*, 2012, pp. 12–18.

[33] Wang, H. Gangarao, R. Liang, and W. Liu, "Durability and prediction models of fiber-reinforced polymer composites under various environmental conditions: A critical review," *Journal of Reinforced Plastics and Composites*, vol. 35, no. 3, pp. 179–211, 2015.

[34] A. Serbescu, M. Guadagnini, and K. Pilakoutas, "Mechanical Characterization of Basalt FRP Rebars and Long-Term Strength Predictive Model," *Journal of Composites for Construction*, vol. 19, no. 2, pp. 265–322, 2015.

[35] H. El-Hassan, T. El-Maaddawy, A. Al-Sallamin, and A. Al-Saidy, "Performance evaluation and microstructural characterization of GFRP bars in seawater-contaminated concrete," *Construction and Building Materials*, vol. 147, pp. 66–78, 2017.

[36] Z. Wang, X. Zhao, G. Xian, G. Wu, R. S. Raman, S. Al-Saadi, and A. Haque, "Long-term durability of basalt- and glass-fibre reinforced polymer (BFRP/GFRP) bars in seawater and sea sand concrete environment," *Construction and Building Materials*, vol. 139, no. 2, pp. 467–489, 2017.

[37] Y. Fang, K. Wang, D. Hui, F. Xu, W. Liu, S. Yang, and L. Wang, "Monitoring of seawater immersion degradation in glass fibre reinforced polymer composites using quantum dots," *Composites Part B: Engineering*, vol. 112, pp. 93–102, 2017.

[38] J. F. Davalos, Y. Chen, and I. Ray, "Long-term durability prediction models for GFRP bars in concrete environment," *Journal of Composite Materials*, vol. 46, no. 16, pp. 1899–1914, 2011.

[39] H. Li, G. Xian, M. Minglei, and W. Jingyu, "Durability and Fatigue Performances of Basalt Fiber /Epoxy Reinforcing Bars," in *5th International Conference on FRP Composites in Civil Engineering*, 2012, pp. 12–33.

[40] B. Benmokrane, *GFRP Durability Study Report*. University of Sherbooke, 2005.

[41] J. J. Lee, J. Song, and H. Kim, "Chemical stability of basalt fiber in alkaline solution," *Fibers and Polymers*, vol. 15, no. 11, pp. 2329–2334, 2014.

[42] M. Robert and B. Benmokrane, "Physical, Mechanical, and Durability Characterization of Preloaded GFRP Reinforcing Bars," *Journal of Composites for Construction*, vol. 14, no. 4, pp. 368–375, 2010.

[43] ASTM C597 – 16, *Standard Test Method for Pulse Velocity Through Concrete*. ASTM International: West Conshohocken, PA, 2016.

[44] ASTM C597, *Standard test method for pulse velocity through concrete*. ASTM International, USA, 2016.
[45] ASTM C496, *Standard test method for splitting tensile strength of cylindrical concrete specimens*. ASTM International, USA, 2011.
[46] ASTM E70-07, *Standard Test Method for pH of Aqueous Solutions with the Glass Electrode*. ASTM International, West Conshohocken, PA, 2015.
[47] ASTM C39 / C39M-17a, *Standard Test Method for Compressive Strength of Cylindrical Concrete Specimens*. ASTM International, West Conshohocken, PA, 2017.
[48] ASTM D570, *Standard test method for water absorption of plastics*. ASTM International, USA, 2010.
[49] A. Khalid, B. Sahari, and Y. Khalid, "Environmental effects on the progressive crushing of cotton and glass fiber/epoxy composite cones," *Advanced in Materials Processing and Technologies*, vol. 11, no. 3, pp. 680-689, 2004.
[50] F. Abed, M. Saffarini, A. Abdul-Latif, and G. Voyiadjis, "Flow Stress and Damage Behavior of C45 Steel Over a Range of Temperatures and Loading Rates," *Journal of Engineering Materials and Technology*, vol. 139, no. 2, pp. 523–588, 2017.
[51] ASTM D3418-15, *Standard Test Method for Transition Temperatures and Enthalpies of Fusion and Crystallization of Polymers by Differential Scanning Calorimetry*. ASTM International, West Conshohocken, PA, 2015.
[52] ASTM E1356, *Standard test method for assignment of the glass transition temperatures by differential scanning calorimetry*. ASTM International, USA, 2008.
[53] S. Foster, and L. Bisby, "High temperature residual properties of externally bonded FRP systems," in *Proceedings of the 7th international symposium on fiber reinforced polymer reinforcement for reinforced concrete structures (FRPRCS-7)*, 2005, pp. 12-16.
[54] B. Smith, *Fourier transform infrared spectroscopy*. CRC, Boca Raton, FL, 1996.
[55] A. Mourad, B. M. Abdel-Magid, T. El-Maaddawy, and M. E. Grami, "Effect of Seawater and Warm Environment on Glass/Epoxy and Glass/Polyurethane Composites," *Applied Composite Materials*, vol. 17, no. 5, pp. 557–573, 2010.

Vita

Mohamad Alrifai was born in 1994, in Dubai, United Arab Emirates. He received his primary and secondary education in Dubai, UAE. He received his B.Sc. degree in Civil Engineering from the University of Sharjah in 2016. From 2017 to 2019, he worked as a Civil Engineer in Azizi Developments

In September 2016, he joined the Civil Engineering master's program in the American University of Sharjah as a graduate teaching assistant. His research interests are in Durability, Concrete technology, Mechanics of Materials, Sustainability of Structures.